Reactions of 16-Electron Cp′M(NO)R_2 Complexes of Molybdenum and Tungsten with Water[1]

Peter Legzdins,* Penelope J. Lundmark, Everett C. Phillips, Steven J. Rettig, and John E. Veltheer

Department of Chemistry, The University of British Columbia, Vancouver, British Columbia, Canada V6T 1Z1

Received May 15, 1992

The hydrolytic instability of Cp′Mo(NO)R_2 complexes (Cp′ = Cp (η^5-C_5H_5), Cp* (η^5-C_5Me_5); R = alkyl, aryl) becomes evident during attempts to synthesize them by procedures which have previously afforded the congeneric tungsten species. Thus, treatment of Cp*Mo(NO)I_2 with 2 equiv of Me_3SiCH_2MgCl in Et_2O at room temperature results in the formation of three organometallic complexes which are separable by chromatography on alumina. These products are (a) the expected alkylation product, i.e. the 16-valence-electron dialkyl complex Cp*Mo(NO)(CH_2SiMe_3)$_2$ (1), (b) a novel bimetallic bridging-oxo complex, [Cp*Mo(NO)(CH_2SiMe_3)]$_2$(μ-O) (2), formed by hydrolysis of 1 during workup, and (c) a dimeric reduction product of the starting material, namely [Cp*Mo(NO)I]$_2$ (3). Each of the complexes 1–3 has been fully characterized by conventional spectroscopic methods, and a single-crystal X-ray crystallographic analysis of 2 has also been performed. Crystal data for 2: triclinic, space group $P\bar{1}$, a = 11.7721 (7) Å, b = 16.373 (1) Å, c = 18.161 (1) Å, α = 84.947 (5)°, β = 89.974 (4)°, γ = 83.367 (4)°, Z = 4, D_c = 1.367 g cm^{-3}. The structure was solved by standard heavy-atom methods and was refined by full-matrix least-squares procedures to R_F = 0.025 and R_{wF} = 0.038 for 12 489 reflections having $I \geq 3\sigma(I)$. The most chemically interesting feature about the solid-state molecular structure of 2 is the orthogonal orientation of the two Cp*Mo(NO)(CH_2SiMe_3) units about the essentially linear Mo–O–Mo grouping, an aspect consistent with the existence of multiple bonding in this linkage. Five analogues of 2 have been synthesized by the hydrolysis of several Cp′Mo(NO)R_2 precursors (i.e. Cp′ = Cp, R = CH_2SiMe_3; Cp′ = Cp*, R = CH_2CMe_3, CH_2CMe_2Ph, *o*-tolyl, Ph). These transformations of Cp′M(NO)R_2 to [Cp′M(NO)R]$_2$(μ-O) are quite general for M = molybdenum but do not occur at all for M = tungsten when R = alkyl. Related Cp*W(NO)(aryl)$_2$ complexes (i.e. aryl = Ph, *p*-tolyl, and *o*-tolyl) are converted to their aryl dioxo derivatives Cp*W(O)$_2$(aryl) when exposed to water. Clearly, the reactivity of the 16-electron dialkyl and diaryl complexes of molybdenum with water is fundamentally different from that exhibited by the congeneric tungsten compounds. The reactivities of both the molybdenum and tungsten complexes toward water are discussed in detail.

Introduction

A fundamental theme of our recent research efforts has been the determination of the distinctive physical and chemical properties that the 14-valence-electron fragments Cp′M(NO) (Cp′ = Cp (η^5-C_5H_5), Cp* (η^5-C_5Me_5); M = Mo, W) impart to their complexes. Our task has been complicated somewhat by the fact that these properties are generally dependent on the natures of the metal, the cyclopentadienyl ring, and the ancillary ligands. For instance, the thermal stability order of this family of complexes appears to be W > Mo, Cp* > Cp, and alkyl > aryl, with CpMo(NO)(aryl)$_2$ having yet to be isolated.[1,2] Nevertheless, the most profound differences are imparted by the metal. Thus, we note the following.

(1) Treatment of Cp′M(NO)R_2 complexes with dihydrogen under appropriate experimental conditions produces new types of remarkably thermally stable alkyl hydride complexes if M = W.[3] No such complexes have yet been isolated in the case of M = Mo.

(2) For electronic reasons, the Cp′M(NO) fragments prefer to bind acyclic, conjugated dienes in a twisted, transoidal fashion if M = Mo.[4] Interestingly, the synthetic methodology which produces these Cp′Mo(NO)(η^4-*trans*-diene) complexes fails to afford the congeneric tungsten species.[4c]

We now report the reactivity of typical Cp′M(NO)R_2 (M = Mo, W; R = alkyl, aryl) complexes toward water which provides the clearest illustration to date of this pronounced dependence on M. In general, the W–R σ-bonds in the tungsten alkyl compounds are stable and are not easily hydrolyzed. The isolable Cp′W(NO)(aryl)$_2$ complexes, on the other hand, are converted to their aryl dioxo analogues Cp′W(O)$_2$(aryl) when exposed to water.[5] In contrast, the Mo–R σ-bonds in *all* (both alkyl and aryl) isolable Cp′Mo(NO)R_2 complexes are readily hydrolyzed to form bimetallic complexes of the type [Cp′Mo(NO)R]$_2$(μ-O) and free hydrocarbon. In this paper we focus primarily on these molybdenum systems and present the synthesis, characterization, and some reactivity of several of these new oxo-bridged dimolybdenum complexes, which are the first organometallic nitrosyl complexes of this type to have been reported. We also effect a comparison of the reactivities of the various Cp′M(NO)R_2 complexes with water, since knowledge about such processes is of fundamental significance, given that there is relatively little known at present about the reactions of transition-metal–carbon σ-bonds with H_2O.[6]

Experimental Section

All reactions and subsequent manipulations involving organometallic reagents were performed under anaerobic and anhydrous conditions using an atmosphere of prepurified dinitrogen

(1) Organometallic Nitrosyl Chemistry. 54. Part 53: Dryden, N. H.; Legzdins, P.; Rettig, S. J.; Veltheer, J. E. *Organometallics*, in press.

(2) The most notable example of a thermally unstable Cp′M(NO)R_2 species is CpMo(NO)(CH_2CMe_3)$_2$; see: Legzdins, P.; Rettig, S. J.; Veltheer, J. E. *J. Am. Chem. Soc.*, in press.

(3) (a) Legzdins, P.; Martin, J. T.; Einstein, F. W. B.; Jones, R. H. *Organometallics* **1987**, *6*, 1826 and references cited therein. (b) Debad, J. D.; Legzdins, P.; Batchelor, R. J.; Einstein, F. W. B. *Organometallics* **1992**, *13*, 6.

(4) (a) Hunter, A. D.; Legzdins, P.; Nurse, C. R.; Einstein, F. W. B.; Willis, A. C. *J. Am. Chem. Soc.* **1985**, *107*, 1791. (b) Hunter, A. D.; Legzdins, P.; Einstein, F. W. B.; Willis, A. C.; Bursten, B. E.; Gatter, M. G. *J. Am. Chem. Soc.* **1986**, *108*, 3843. (c) Christensen, N. J.; Hunter, A. D.; Legzdins, P. *Organometallics* **1989**, *8*, 930.

(5) A notable exception to this generalization is CpW(NO)(*o*-tolyl)$_2$, which is converted to both its arylimido oxo structural isomer, CpW(N-*o*-tolyl)(O)(*o*-tolyl), and its aryl dioxo analogue, CpW(O)$_2$(*o*-tolyl), when exposed as a solid to water vapor: Legzdins, P.; Rettig, S. J.; Ross, K. J.; Veltheer, J. E. *J. Am. Chem. Soc.* **1991**, *113*, 4361.

(6) See for example: *The Chemistry of the Metal-Carbon Bond*; Hartley, F. R., Patai, S., Eds.; Wiley: New York, 1985; Vol. 2.

0276-7333/92/2311-2991$03.00/0

Table I. Numbering Scheme and Elemental Analysis Data for Complexes 1–11

complex	compd no.	anal. found (calcd) C	H	N
$Cp^*Mo(NO)(CH_2SiMe_3)_2$	1	49.74 (49.63)	8.52 (8.57)	3.44 (3.21)
$[Cp^*Mo(NO)(CH_2SiMe_3)]_2(\mu\text{-}O)$	2	47.07 (47.16)	7.64 (7.35)	3.85 (3.93)
$[Cp^*Mo(NO)I]_2$	3	31.02 (30.95)	3.94 (3.90)	3.58 (3.61)
$[CpMo(NO)(CH_2SiMe_3)]_2(\mu\text{-}O)$	4	38.03 (37.76)	5.51 (5.63)	5.00 (4.89)
$[Cp^*Mo(NO)(CH_2CMe_3)]_2(\mu\text{-}O)$	5	53.00 (52.94)	7.74 (7.70)	3.95 (4.12)
$[Cp^*Mo(NO)(CH_2CMe_2Ph)]_2(\mu\text{-}O)$	6	59.33 (59.69)	7.15 (7.01)	3.23 (3.48)
$[Cp^*Mo(NO)(o\text{-tolyl})]_2(\mu\text{-}O)$	7	56.68 (56.67)	6.28 (6.15)	3.77 (3.89)
$[Cp^*Mo(NO)(Ph)]_2(\mu\text{-}O)$	8	54.73 (55.50)	5.81 (5.82)	4.00 (4.04)
$Cp^*W(O)_2Ph$	9	44.93 (44.88)	4.68 (4.71)	0.00 (0.00)
$Cp^*W(O)_2(p\text{-tolyl})$	10	46.03 (46.17)	5.05 (5.01)	0.00 (0.00)
$Cp^*W(O)_2(o\text{-tolyl})$	11	46.65 (46.17)	5.11 (5.01)	0.00 (0.00)

Table II. Mass Spectral and Infrared Data for Complexes 1–11

compd no.	MS, m/z[a]	temp,[b] °C	IR, cm^{-1} ν_{NO}	ν_{Mo-O}	$\nu_{W=O}$
1	437 [P^+]	100	1595		
2	716 [P^+]	120	1576	774	
	686 [P^+ – NO]		1561	750	
3	780 [P^+]	180	1579		
	750 [P^+ – NO]				
4	557 [P^+ – Me]	150	1603	812	
5	680 [P^+]	200	1582	768	
	609 [P^+ – CH_2CMe_3]		1566		
6	805 [P^+]	100	1578	774	
			1564		
7	720 [P^+]	225	1584	771	
	602 [P^+ – NO – tolyl]		1576	743	
			1568		
8	692 [P^+]	100	1589	803	
	662 [P^+ – NO]		1575	785	
			1554		
9	428 [P^+]	120			938
					900
10	442 [P^+]	100			939
					901
11	442 [P^+]	100			940
					899

[a] m/z values are for the highest intensity peak of the calculated isotopic cluster. [b] Probe temperatures.

or argon. Conventional Schlenk techniques and a Vacuum Atmospheres Dri-Lab Model HE-43-2 drybox were employed for the manipulation of air- and moisture-sensitive compounds.[7,8] General procedures routinely employed in these laboratories have been described in detail previously.[9] All reagents were purchased from commercial suppliers or were prepared according to published procedures. Thus, $CpMo(NO)X_2$ and $Cp^*Mo(NO)X_2$ (X = Cl,[10] I[11]) and $CpMo(NO)(CH_2SiMe_3)_2$[12] were prepared by the referenced procedures, and their purities were verified by elemental analyses. Some Grignard reagents employed, namely Me_3SiCH_2MgCl (1.0 M in Et_2O), PhMgCl (1.0 M in THF), and (*o*-tolyl)MgCl (1.0 M in THF) were purchased from Aldrich Chemical Co. and were used as received. The diaryl complexes $Cp^*W(NO)(aryl)_2$ (aryl = Ph, *p*-tolyl, *o*-tolyl) were prepared by treatment of $Cp^*W(NO)Cl_2$ with the appropriate $(aryl)_2Mg(dioxane)_x$ reagent in THF.[1] Other organomagnesium reagents, namely $(Me_3CCH_2)_2Mg$, $(PhMe_2CCH_2)_2Mg$, and Ph_2Mg, were synthesized by using a method similar to that described in the literature for the synthesis of $(Me_3SiCH_2)_2Mg$.[1,10,13] D_2O (MSD Isotopes) and $^{18}OH_2$ (Aldrich) were used as received. Solvents were dried according to conventional procedures,[14] distilled, and deaerated with argon prior to use.

The column chromatography materials used during this work were alumina (80–200 mesh, Fisher neutral, Brockman activity I), alumina I deactivated to alumina III with 6% w/w deaerated water, and Florisil (60–100 mesh, Fisher). Filtrations were performed through Celite 545 diatomaceous earth (Fisher) that had been oven-dried and cooled in vacuo.

Infrared spectra were recorded on a Nicolet 5DX FT-IR spectrometer which was internally calibrated with a He/Ne laser. All ^1H and ^{13}C NMR spectra were obtained on a Varian Associates XL-300 spectrometer, and the chemical shifts of the observed resonances are reported in parts per million (ppm) downfield from Me_4Si. Residual solvent peaks used as internal standards were as follows: C_6D_6, 7.15 ppm (^1H) or natural-abundance carbon signal at 128.0 ppm (^{13}C); CD_2Cl_2, 5.32 ppm (^1H) or natural-abundance carbon signal at 53.8 ppm (^{13}C); THF-d_8, 3.58 ppm (^1H). Ms. M. Austria, Ms. L. Darge, and Dr. S. O. Chan assisted in the collection of some of the NMR spectra. The C_6D_6 used in this work was dried over activated 4-Å molecular sieves and filtered through glass wool before use. Other deuterated solvents were used as received. Low-resolution mass spectra were recorded at 70 eV using the direct-insertion method on an Atlas CH4B or a Kratos MS50 spectrometer by Dr. G. K. Eigendorf and the staff of the UBC Mass Spectrometry Laboratory; probe temperatures were between 100 and 225 °C. Elemental analyses were performed by Mr. P. Borda of this department.

Electrochemical Measurements. The customary methodology employed during cyclic voltammetry (CV) studies in these laboratories has been described in detail elsewhere.[15] The potentials were supplied by a BAS CV27 voltammograph, and the resulting cyclic voltammograms were recorded on a Hewlett-Packard Model 7090A X-Y recorder in the buffered recording mode. The three-electrode cell consisted of a Pt-bead working electrode (~1-mm diameter), a coiled Pt-wire auxiliary electrode, and a Ag-wire reference electrode. THF (BDH, OmniSolv grade) was twice distilled from CaH_2 and then vacuum-transferred from sodium benzophenone. Solutions were prepared in the glovebox at 0.10 M in the $[n\text{-}Bu_4N]PF_6$ support electrolyte and $\sim 6 \times 10^{-4}$ M in the organometallic complex to be studied. The formal oxidation potentials, $E^{\circ\prime}$, for reversible couples are defined as the average of the cathodic and anodic peak potentials, $(E_{p,c} + E_{p,a})/2$, and are reported versus the Ag-wire reference electrode. ΔE is defined by $|E_{p,c} - E_{p,a}|$, and the cathodic to anodic peak current ratio is given by $i_{p,c}/i_{p,a}$. The linearity of a plot of $i_{p,c}$ vs $v^{1/2}$ was checked for redox processes to establish the existence of diffusion control. Compensation for iR drop in potential measurements was not employed during this study. Ferrocene was used as an internal reference during this work, with the redox couple Cp_2Fe/Cp_2Fe^+ occurring at $E^{\circ\prime} = 0.53$ V versus Ag wire in THF over the range of scan rates used (0.10–0.80 V s^{-1}). The anodic and cathodic peak separation (ΔE) for this couple increases with increasing scan rate (90–260 mV between 0.10 and 0.80 V s^{-1}), but since the Cp_2Fe/Cp_2Fe^+ couple is known to be highly reversible, other redox couples exhibiting similar peak separations to the internal standard were also considered to be electrochemically reversible. The ratio of cathodic to anodic peak current, $i_{p,c}/i_{p,a}$, for the oxidation of ferrocene was unity over all scan rates (v) used, as expected for a chemically reversible process.

Reaction of $Cp^*Mo(NO)I_2$ with Me_3SiCH_2MgCl. To a stirred, purple suspension of $Cp^*Mo(NO)I_2$ (3.00 g, 5.83 mmol) in Et_2O (200 mL) was added dropwise from an addition funnel

(7) Shriver, D. F.; Drezdzon, M. A. *The Manipulation of Air-Sensitive Compounds*, 2nd ed.; Wiley-Interscience: Toronto, 1986.
(8) Wayda, A. L.; Darensbourg, M. Y. *Experimental Organometallic Chemistry: A Practicum in Synthesis and Characterization*; ACS Symposium Series 357; American Chemical Society: Washington, DC, 1987.
(9) Legzdins, P.; Jones, R. H.; Phillips, E. C.; Yee, V. C.; Trotter, J.; Einstein, F. W. B. *Organometallics* **1991**, *10*, 986.
(10) Dryden, N. H.; Legzdins, P.; Batchelor, R. J.; Einstein, F. W. B. *Organometallics* **1991**, *10*, 2077.
(11) (a) Nurse, C. R. Ph.D. Dissertation, The University of British Columbia, 1983. (b) James, T. A.; McCleverty, J. A. *J. Chem. Soc. A* **1971**, 1068.
(12) Legzdins, P.; Rettig, S. J.; Sánchez, L. *Organometallics* **1988**, *7*, 2394.
(13) (a) Anderson, R. A.; Wilkinson, G. *J. Chem. Soc., Dalton Trans.* **1977**, 809. (b) Anderson, R. A.; Wilkinson, G. *Inorg. Synth.* **1979**, *19*, 262.
(14) Perrin, D. D.; Armarego, W. L. F.; Perrin, D. R. *Purification of Laboratory Chemicals*, 3rd ed.; Pergamon Press: Oxford, U.K., 1988.
(15) Herring, F. G.; Legzdins, P.; Richter-Addo, G. B. *Organometallics* **1989**, *8*, 1485 and references cited therein.

Table III. ^1H and $^{13}C\{^1H\}$ NMR Data (C_6D_6) for Complexes 1–11

compd no.	^1H NMR, δ	$^{13}C\{^1H\}$ NMR, δ
1	2.21 (d, 2 H, J_{HH} = 10.8 Hz, $CH_AH_XSiMe_3$), 1.49 (s, 15 H, $C_5(CH_3)_5$), 0.37 (s, 18 H, 2 × $Si(CH_3)_3$), −1.17 (d, 2 H, J_{HH} = 10.8 Hz, $CH_ACH_XSiMe_3$)	110.52 ($C_5(CH_3)_5$), 66.54 (CH_2SiMe_3), 9.97 ($C_5(CH_3)_5$), 2.59 ($CH_2Si(CH_3)_3$)
2	isomer A (90%): 1.59 (s, 30 H, $C_5(CH_3)_5$), 0.84 (d, 2 H, J_{HH} = 12.3 Hz, $CH_AH_BSiMe_3$), 0.75 (d, 2 H, J_{HH} = 12.3 Hz, $CH_AH_BSiMe_3$), 0.45 (s, 18 H, 2 × $Si(CH_3)_3$) isomer B (10%): 1.71 (s, 30 H, $C_5(CH_3)_5$), methylene protons not obsd, 0.42 (s, 18 H, 2 × $Si(CH_3)_3$)	isomer A: 112.60 ($C_5(CH_3)_5$), 36.50 (CH_2SiMe_3), 9.96 ($C_5(CH_3)_5$), 2.83 ($CH_2Si(CH_3)_3$) isomer B: 113.50 ($C_5(CH_3)_5$), 36.20 (CH_2SiMe_3), 10.26 ($C_5(CH_3)_5$), 3.43 ($CH_2Si(CH_3)_3$)
3	1.92 (s, $C_5(CH_3)_5$)	108.90 ($C_5(CH_3)_5$), 12.58 ($C_5(CH_3)_5$)
4[a]	isomer A (75%): 5.32 (s, 10 H, C_5H_5), 1.80 (s, 4 H, CH_2SiMe_3), 0.34 (s, 18 H, $Si(CH_3)_3$) isomer B (25%): 5.42 (s, 10 H, C_5H_5), 2.14 (d, 2 H, J_{HH} = 10.6 Hz, $CH_AH_XSiMe_3$), 1.48 (d, 2 H, J_{HH} = 10.6 Hz, $CH_AH_XSiMe_3$), 0.42 (s, 18 H, 2 × $Si(CH_3)_3$)	isomer A: 104.60 (C_5H_5), 39.30 (CH_2SiMe_3), 2.23 ($Si(CH_3)_3$) isomer B: 104.55 (C_5H_5), 39.20 (CH_2SiMe_3), 1.36 ($Si(CH_3)_3$)
5	isomer A (100%): 1.80 (d, 2 H, J_{HH} = 13.2 Hz, $CH_AH_BCMe_3$), 1.74 (d, 2 H, J_{HH} = 13.2 Hz, $CH_AH_BCMe_3$), 1.63 (s, 30 H, $C_5(CH_3)_5$), 1.45 (s, 18 H, 2 × $C(CH_3)_3$)	isomer A: 112.44 ($C_5(CH_3)_5$), 68.06 ($C(CH_3)_3$), 33.89 (CH_2CMe_3), 28.05 ($C(CH_3)_3$), 9.81 ($C_5(CH_3)_5$)
6	isomer A (100%): 7.71 (d, 4 H, ortho protons), 7.32 (t, 4 H, meta protons), 7.10 (t, 2 H, para protons), 2.18 (d, 2 H, J_{HH} = 12.4 Hz, $CH_AH_BCMe_2Ph$), 2.04 (d, 2 H, J_{HH} = 12.4 Hz, $CH_AH_BCMe_2Ph$), 1.84 (s, 6 H, $CH_2C(CH_3)_A(CH_3)_BPh$), 1.78 (s, 6 H, $CH_2C(CH_3)_A(CH_3)_BPh$), 1.56 (s, 30 H, $C_5(CH_3)_5$)	isomer A: 155.42 (C_{ipso}), 128.40 (C_{phenyl}), 125.91 (C_{phenyl}), 125.34 (C_{phenyl}), 112.83 ($C_5(CH_3)_5$), 69.91 ($CH_2C(CH_3)_2Ph$), 43.78 ($CH_2C(CH_3)_2Ph$), 32.02 ($(CH_3)_A$, 30.77 ($(CH_3)_B$, 9.76 ($C_5(CH_3)_5$)
7	isomer A (65%): 7.80–7.05 (m, 8 H, aryl H), 2.40 (s, 6 H, aryl CH_3), 1.59 (s, 30 H, $C_5(CH_3)_5$) isomer B (35%): 7.80–7.05 (m, 8 H, aryl H), 2.29 (s, 6 H, aryl CH_3), 1.62 (s, 30 H, $C_5(CH_3)_5$)	
8	isomer A (97%): 7.77 (d, 4 H, ortho protons), 7.31 (t, 4 H, meta protons), 7.21 (m, 2 H, para protons), 1.56 (s, 30 H, $C_5(CH_3)_5$) isomer B (3%): 1.62 (s, 30 H, $C_5(CH_3)_5$), other signals not obsd	isomer A: 178.10 (C_{ipso}), 135.30 (C_{ortho}), 127.50 (C_{meta}), 127.21 (C_{para}), 114.45 ($C_5(CH_3)_5$), 9.69 ($C_5(CH_3)_5$) isomer B: signals not obsd
9	7.52–7.46 (m, 2 H, ortho protons), 7.12–6.98 (m, 3 H, other aryl protons), 1.66 (s, 15 H, $C_5(CH_3)_5$)	
10[b]	7.21 (d, 2 H, J = 10.1 Hz, aryl protons), 7.11 (d, 2 H, J = 10.1 Hz, aryl protons), 2.30 (s, 3 H, para CH_3), 2.01 (s, 15 H, $C_5(CH_3)_5$)	C_{ipso} not obsd, 141.15 (C_{ortho}), 141.01 (C_{para}), 129.69 (C_{meta}), 119.40 ($C_5(CH_3)_5$), 21.52 (para CH_3), 11.03 ($C_5(CH_3)_5$)
11	7.58 (dd, 1 H, J = 7.5, 1.5 Hz, ortho proton), 7.20 (d, 1 H, J = 7.8 Hz, aryl proton), 7.04 (m, 1 H, aryl proton), 6.95 (m, 1 H, aryl proton), 2.26 (s, 3 H, ortho CH_3), 1.67 (s, 15 H, $C_5(CH_3)_5$)	

[a] Relaxation delays (20 s) were required to observe full integration of Cp proton signals. [b] Both spectra recorded in CD_2Cl_2.

an Et_2O solution of Me_3SiCH_2MgCl (12.0 mL of a 1.0 M solution, 12.0 mmol). The reaction mixture immediately became dark green and then slowly turned purple while a greenish white precipitate deposited. After being stirred for 1 h, the mixture was treated with 0.3 mL of deaerated H_2O. Although the solution remained purple, the green precipitate disappeared and a white gelatinous precipitate formed. The solvent was removed under reduced pressure until approximately 10 mL remained, at which point the mixture was filtered onto an alumina III column (3 × 6 cm) made up in hexanes. Elution of the column with Et_2O developed a purple band which slowly turned red-brown as it passed through the column. The red-brown eluate was collected and taken to dryness in vacuo, and the residue was fractionally crystallized from 1:1 Et_2O/hexanes at −20 °C to obtain 0.050 g (2% yield) of purple Cp*Mo(NO)$(CH_2SiMe_3)_2$ (1) and 0.080 g (4% yield) of red-black [Cp*Mo(NO)$(CH_2SiMe_3)]_2(\mu$-O) (2). The column was then washed with CH_2Cl_2 until the washings were colorless (ca. 100 mL). The volume of the deep red washings was reduced in vacuo to one-third, and an equal volume of hexanes was added. Further concentration under reduced pressure induced the crystallization of 0.62 g (27% yield) of orange [Cp*Mo(NO)I]$_2$ (3). The low isolated yields of complexes 1–3 obtained from the reaction mixture reflect the inherent difficulty in separating them by chromatography and fractional crystallization.

Preparation of Cp*Mo(NO)$(CH_2SiMe_3)_2$ (1). The procedure outlined below is a significant improvement of the methodology that we employed previously to synthesize this compound.[16] The main point is that Cp*Mo(NO)$(CH_2SiMe_3)_2$ can only be synthesized reproducibly in preparative amounts by employing Cp*Mo(NO)Cl_2 and a slight deficiency of Me_3SiCH_2MgCl under rigorously anhydrous experimental conditions.

To a rapidly stirred, brown suspension of Cp*Mo(NO)Cl_2 (4.58 g, 13.8 mmol) in Et_2O (200 mL), maintained at −60 °C using an acetone/dry-ice bath, was added Me_3SiCH_2MgCl (27.4 mL of a 1.0 M Et_2O solution, 27.4 mmol) in a dropwise fashion from an addition funnel under a constant purge of Ar. Immediately, the reaction mixture turned purple, and an off-white precipitate slowly formed. The reaction mixture was stirred while the cold bath was warmed slowly to room temperature over 2 h (ν_{NO} = 1593 cm^{-1}). The final deep purple reaction mixture was taken to dryness in vacuo. Under rigorously anaerobic conditions, the remaining lavender solid was suspended in hexanes (50 mL), and the resulting slurry was filtered through Celite (3 × 3 cm) on a medium-porosity frit. The Celite plug was then rinsed with hexanes (2 × 15 mL). The combined, deep purple filtrates were taken to dryness and extracted with pentane (3 × 15 mL). Cooling of the pentane extracts for 2 days at −30 °C in a freezer induced the deposition of very large (e.g. 10 mm × 5 mm × 2 mm) violet crystals. These crystals (2.55 g) were collected by filtration. Further concentration of the filtrate and cooling afforded a second crop of crystals (1.08 g). The total yield of 1 thus obtained was 3.63 g (60%), and the complex was stored in a freezer.

Preparation of [Cp*Mo(NO)$(CH_2SiMe_3)]_2(\mu$-O) (2). A solution of 1 generated from Cp*Mo(NO)Cl_2 (1.18 g, 3.55 mmol) and Me_3SiCH_2MgCl (8.0 mL of a 1.0 M Et_2O solution, 8.0 mmol) in Et_2O (150 mL) was prepared. Treatment of the resultant purple solution with deaerated H_2O (0.20 mL) destroyed any excess

(16) Legzdins, P.; Phillips, E. C.; Sánchez, L. *Organometallics* **1989**, *8*, 940.

Grignard reagent and caused the decomposition of Cp*Mo(NO)(CH_2SiMe_3)$_2$ to [Cp*Mo(NO)(CH_2SiMe_3)]$_2$(μ-O) (2; ν_{NO} = 1584 cm^{-1}). The solvent volume was then reduced to approximately 15 mL by slow evaporation of the Et_2O under reduced pressure. At this point the mixture contained mostly 2, but small quantities of 1 persisted in solution. The mixture was then *slowly* chromatographed on an alumina III column (3 × 8 cm) made up in Et_2O using Et_2O as eluant. As the purple band indicative of 1 passed through the column, it changed color, becoming the red-brown color characteristic of 2. The rest of 2 eluted from the column next. The combined red-brown eluates were collected, and their volume was reduced in vacuo until the first signs of crystallization became evident. Maintaining the concentrated solution at −20 °C overnight resulted in the deposition of large red-black crystals (0.65 g, 51% yield) of [Cp*Mo(NO)(CH_2SiMe_3)]$_2$(μ-O), which were collected by filtration. The filtrate was taken to dryness, and the residue was redissolved in hexanes. Crystallization of this second fraction afforded 0.30 g more of 2 for a total yield of 75%.

The conversion of 1 to 2 could be conveniently monitored by ^{1}H NMR spectroscopy, which indicated that the yield of the reaction was >95%. For example, the reaction of Cp*Mo(NO)(CH_2SiMe_3)$_2$ (38 mg) in C_6D_6 (1.2 mL) with H_2O (10 μL, excess) required approximately 2 min at room temperature to go to completion. The signal due to the 2 equiv of Me_4Si formed in the reaction could be easily detected at δ 0.00 ppm.

Preparation of [Cp*Mo(NO)I]$_2$ (3). Cp*Mo(NO)I_2 (0.790 g, 1.53 mmol) was dissolved in THF (20 mL), and the resulting solution was cooled to −20 °C. In another flask Zn metal (0.050 g, 0.765 mmol) was amalgamated with Hg (~1 mL), THF (30 mL) was added to the amalgam, and the mixture was cooled to −20 °C. The cold THF solution of Cp*Mo(NO)I_2 was then cannulated onto the amalgam. The mixture was stirred vigorously for 2 h while the reaction mixture was warmed to room temperature. The final deep red supernatant solution was decanted from the Hg and was taken to dryness. The residue was extracted with CH_2Cl_2 (3 × 10 mL) to obtain an orange solution that was filtered through an alumina I column (2 × 5 cm) supported on a medium-porosity frit. The volume of the combined filtrates was reduced to 5 mL in vacuo, and hexanes (5 mL) was added. Maintaining this solution at −30 °C for 3 days induced the crystallization of 0.20 g (34% yield) of 3 as a red-orange microcrystalline solid, which was collected by filtration. The use of excess Zn in the above procedure was detrimental and lowered the final yield of 3 substantially. Furthermore, the reaction of Cp*Mo(NO)I_2 with water did not produce complex 3.

Preparation of [CpMo(NO)(CH_2SiMe_3)]$_2$(μ-O) (4). This complex was prepared in 57% yield from CpMo(NO)Cl_2 and Me_3SiCH_2MgCl in a manner identical with that described above for complex 2, except that final purification of 4 was effected by crystallization from hexanes.

Preparation of [Cp*Mo(NO)(CH_2CMe_3)]$_2$(μ-O) (5). Solid Cp*Mo(NO)Cl_2 (0.498 g, 1.50 mmol) and solid (Me_3CCH_2)$_2$Mg (0.510 g, 3.00 mmol of $Me_3CCH_2^-$) were intimately mixed in a Schlenk tube. The tube was cooled to −80 °C, and THF (20 mL) was added. When the temperature was raised to −20 °C, the solution became orange-red (ν_{NO} = 1588 cm^{-1}), a feature indicative of the formation of Cp*Mo(NO)(CH_2CMe_3)$_2$. The reaction mixture was maintained at temperatures below 0 °C as the solvent was removed in vacuo. The remaining red solid was then suspended in Et_2O (20 mL). While this suspension was being rapidly stirred, deaerated water (0.7 mL) was added, thereby producing a red solution and a brown precipitate. After 15 min, the mixture was filtered through a column of alumina I (3 × 3 cm), and the column was rinsed with Et_2O (75 mL). The combined filtrates were taken to dryness. The red solid was dissolved in THF (5 mL), and water (0.5 mL) was added. The mixture was stirred for 6 h, whereupon it was filtered through a column of alumina I (2 × 6 cm) supported on a frit. The filtrate was taken to dryness, and the residue was crystallized from hexanes/Et_2O (5:1) to obtain black crystals of 5 (0.45 g, 1.32 mmol, 88%).

Preparation of [Cp*Mo(NO)(CH_2CMe_2Ph)]$_2$(μ-O) (6). Solid Cp*Mo(NO)Cl_2 (0.664 g, 2.00 mmol) and solid ($PhMe_2CCH_2$)$_2$Mg (0.398 g, 3.90 mmol of $PhMe_2CCH_2^-$) were intimately mixed in a Schlenk tube. The tube was cooled to −80 °C, and THF (20 mL) was added. Upon being warmed to −20 °C, the solution became red (ν_{NO} = 1586 cm^{-1}), thereby indicating the formation of Cp*Mo(NO)(CH_2CMe_2Ph)$_2$. The solution was warmed to room temperature and stirred for 1 h, and then the solvent was removed in vacuo. The residues were suspended in Et_2O/hexanes (50 mL, 4:1 mixture), the suspension was stirred vigorously, and deaerated water (0.40 mL) was added. The solution quickly became deep red, and an oily beige precipitate formed on the sides of the Schlenk tube. After 10 min the reaction mixture was filtered through alumina I (2 × 6 cm) supported on a frit. Removal of the solvent from the filtrate left a red oil. This oil was dissolved in pentane and transferred to an alumina I (2 × 4 cm) column supported on a frit. The column was washed with pentane (100 mL), and the washes were discarded. Complex 6 was then removed from the column with Et_2O (100 mL). Solvent was removed from the red Et_2O filtrate, and the residue was dried in vacuo (5 × 10^{-3} Torr) for 48 h at 35–40 °C. The red solid thus obtained tended to be somewhat oily, presumably reflecting its contamination with *t*-BuPh. Crystallization of this residue from pentane yielded 0.39 g (50% yield) of analytically pure 6. Subsequent crops of crystals obtained from the supernatant liquid were too oily to be isolated in analytically pure form.

Preparation of [Cp*Mo(NO)(*o*-tolyl)]$_2$(μ-O) (7). Cp*Mo(NO)Cl_2 (0.664 g, 2.00 mmol) was partially dissolved in THF (10 mL) cooled to −50 °C. A single aliquot of (*o*-tolyl)MgCl (4.2 mL of a 1.0 M THF solution, 4.2 mmol) was added via syringe to the dichloride slurry. The resulting purple solution of Cp*Mo(NO)(*o*-tolyl)$_2$ (ν_{NO} = 1601 cm^{-1}) was treated with deaerated water (0.1 mL) at −50 °C. The purple solution changed instantly to red-brown. The volume of the solution was reduced to 3 mL in vacuo, and it was transferred to the top of an alumina III column (2 × 5 cm). A brown band was eluted from the column with acetone and collected in a flask. Slow evaporation of the acetone solvent from the eluate in air afforded 0.51 g (71% yield) of 7 as medium brown microcrystals, which were collected by filtration, washed with pentane (10 mL), and dried in vacuo.

Preparation of [Cp*Mo(NO)(Ph)]$_2$(μ-O) (8). Cp*Mo(NO)Cl_2 (0.332 g, 1.00 mmol) and Ph_2Mg (0.356 g, 2.20 mmol of Ph^-) were intimately mixed in a Schlenk tube. The tube and contents were then cooled to −80 °C, and THF (10 mL) was added. The Schlenk tube and its contents were then quickly warmed to room temperature by immersing the tube for 1 min in a warm-water bath. The violet solution of Cp*Mo(NO)Ph_2 (ν_{NO} = 1615 cm^{-1}) thus produced was taken to dryness, and the residue was redissolved in Et_2O (50 mL) and the solution filtered on Celite (1 × 4 cm). The violet filtrate was cooled to 0 °C and treated with water (50 μL), whereupon the color of the solution changed to red-brown within 1 min. The ether was removed from the final mixture in vacuo, and the residue was crystallized from hexanes/CH_2Cl_2 (1:1) to obtain 0.27 g (78% yield) of 8 as a dark brown microcrystalline solid.

Preparation of Cp*W(O)$_2$(aryl) (aryl = Ph, *p*-Tolyl, and *o*-Tolyl; 9–11). The three aryl dioxo complexes were prepared in a similar manner, the synthesis of Cp*W(O)$_2$(*p*-tolyl) (10) being presented below as a representative example.

A sample of Cp*W(NO)(*p*-tolyl)$_2$ (0.200 g, 0.377 mmol) was dissolved in Et_2O (20 mL). The resulting blue solution was stirred at room temperature, and a single drop of H_2O was added, whereupon the solution became green immediately. The solution was taken to dryness in vacuo, and the brown residue was extracted with Et_2O (5 × 10 mL). The combined extracts were filtered through Florisil (2 × 3 cm), concentrated under reduced pressure, and placed in a freezer overnight. These operations induced the crystallization of 0.070 g (42% yield) of colorless, microcrystalline Cp*W(O)$_2$(*p*-tolyl) (10), which was collected by filtration.

Similarly, Cp*W(O)$_2$Ph (9) and Cp*W(O)$_2$(*o*-tolyl) (11) were obtained in 45 and 80% yield from Cp*W(NO)Ph_2 and Cp*W(NO)(*o*-tolyl)$_2$, respectively. Complexes 9–11 could also be obtained in comparable yields by treatment of their diaryl precursors in the solid state with O_2. All three aryl dioxo complexes are colorless solids which display a high degree of air stability.

Reaction of Cp*Mo(NO)(CH_2SiMe_3)$_2$ (1) with $^{18}OH_2$. Complex 1 (24 mg, 0.055 mmol) was dissolved in C_6D_6 (1.2 mL) and was treated with $^{18}OH_2$ (10 μL). After being shaken vigorously for 2 min, the sample was filtered through a column of Celite (0.3 × 0.5 cm) into an NMR tube to remove the excess $^{18}OH_2$. Ap-

proximately 95% of the signal intensity in the ^1H NMR spectrum of the filtrate was attributable to complex **2**. Two small singlets were observed at δ 1.89 and 1.78 ppm, the latter being attributable to a small amount of $[Cp^*Mo(O)_2]_2(\mu\text{-}O)$.[17] The signal at δ 0.00 ppm confirmed the presence of Me_4Si, the byproduct of the hydrolysis reaction.

Reaction of $Cp^*Mo(NO)(CH_2SiMe_3)_2$ (1) with D_2O. Complex **1** (20 mg, 0.046 mmol) was dissolved in C_6D_6 (1.2 mL) and treated with D_2O (10 μL). After being shaken vigorously for 2 min, the sample was filtered through Celite (0.3 × 0.5 cm) into an NMR tube to remove excess D_2O. The ^1H NMR spectrum of the filtrate revealed the presence of 2 equiv of DH_2CSiMe_3 by its characteristic singlet at δ 0.00 and its 1:1:1 triplet (J_{HD} = 2.1 Hz) at a slightly higher field.

Reaction of $[Cp^*Mo(NO)(CH_2SiMe_3)]_2(\mu\text{-}O)$ (2) with O_2. $[Cp^*Mo(NO)(CH_2SiMe_3)]_2(\mu\text{-}O)$ (0.10 g, 0.14 mmol) was dissolved in hexanes (5 mL). The atmosphere in the flask containing the deep red solution was first evacuated and then pressurized to 1 atm with O_2. After being stirred at room temperature for 24 h, the resulting amber solution was taken to dryness in vacuo. Extraction of the residue with Et_2O and subsequent crystallization afforded yellow-brown crystals of $[Cp^*Mo(O)_2]_2(\mu\text{-}O)$ (43 mg, 56% yield).[17] There was no evidence for any $Cp^*Mo(O)_2(CH_2SiMe_3)$ having been formed.

In related experiments, various solutions of complexes **5** and **8** were allowed to evaporate to dryness in a beaker in the atmosphere. The only organometallic complex detectable in each dried residue by ^1H NMR spectroscopy was $[Cp^*Mo(O)_2]_2(\mu\text{-}O)$.

Reaction of $[Cp^*Mo(NO)(CH_2SiMe_3)]_2(\mu\text{-}O)$ (2) with Excess Water. Treatment of **2** (28 mg) with an excess of water (25 μL) in THF-d_8 (1 mL) for 48 h afforded an amber solution whose ^1H NMR spectrum showed $[Cp^*Mo(O)_2]_2(\mu\text{-}O)$ (δ 1.94) to constitute >95% of the signal intensity. The other principal signals were due to H_2O and Me_4Si.

Kinetic Studies. In general, a standard solution of **1** was prepared in a drybox in a volumetric flask using THF as solvent. Aliquots of this standard solution were diluted as required, and 2 mL of the diluted solution was then quickly mixed with 2 mL of a standard solution of water in THF in a UV–vis spectrophotometer cell equipped with a 4-mm Kontes stopcock. The concentration of the water was sufficiently high such that all runs were effectively conducted under pseudo-first-order conditions. The cell and its contents were shaken, quickly removed from the drybox, and placed in a Hewlett-Packard 8542A diode array spectrometer. The solution was left unstirred and allowed to equilibrate with the spectrometer temperature for 300 s. Spectra were then recorded at regular intervals of 150 s, and data were collected for approximately 1 half-life (i.e. until significant deviations from linearity of the monitored parameters occurred). The absorbance values at infinity were determined by calculation; i.e. the correlation coefficients of pseudo-first-order log plots were optimized by varying the values of A_∞. The observed rate constants (k_{obs}) were then calculated from plots of ln ($A_\infty - A_t$) versus time (in seconds).

X-ray Crystallographic Analysis of $[Cp^*Mo(NO)(CH_2SiMe_3)]_2(\mu\text{-}O)$ (2). The X-ray structure determination of **2** was performed as follows. A suitable crystal was obtained by crystallization of a saturated Et_2O–hexanes solution of **2** at −30 °C for 2 days. After preliminary photographic investigation, the crystal was mounted in a thin-walled glass capillary under N_2 and transferred to an Enraf-Nonius CAD4-F diffractometer equipped with a graphite-monochromated Mo Kα radiation ($\lambda_{K\alpha_1}$ = 0.709 30 Å, $\lambda_{K\alpha_2}$ = 0.713 59 Å). Final unit-cell parameters were obtained by least-squares analysis of (sin 2θ)/λ values for 25 well-centered high-angle reflections with 50.0° ≤ 2θ ≤ 54.6°. The intensities of three standard reflections were measured every 1 h of X-ray exposure time during the data collection and showed no appreciable variations in intensity (ca. 0.5%) with time. The data were processed[18] and corrected for Lorentz and polarization effects and for absorption using the Gaussian integration method.[19,20] A total of 15 828 reflections with $2\theta \le 55°$ were collected, and those 12 489 having $I \ge 3\sigma(I)$ were employed in the solution and refinement of the structure. Pertinent crystallographic and experimental parameters for complex **2** are summarized in Table IV.

Table IV. Crystallographic and Experimental Data for Complex 2[a]

formula	$C_{28}H_{52}Mo_2N_2O_3Si_2$
fw	712.78
habit	prism
cryst size, mm	0.27 × 0.33 × 0.46
cryst syst	triclinic
space group	$P\bar{1}$
a, Å	11.7721 (7)
b, Å	16.373 (1)
c, Å	18.161 (1)
α, deg	84.947 (5)
β, deg	89.975 (4)
γ, deg	83.367 (4)
V, Å^3	3463.3 (4)
Z	4
T, °C	21
D_c, g/cm^3	1.367
F(000)	1480
μ(Mo Kα), cm^{-1}	8.02
transmissn factors	0.747–0.825
scan type	ω–2θ
scan range, deg in ω	0.70 + 0.35 tan θ
scan speed, deg/min	1.7–20.1
data collected	$+h,\pm k,\pm l$
$2\theta_{max}$, deg	55
cryst decay	negligible
no. of unique rflns	15 828
no. of rflns with $I \ge 3\sigma(I)$	12 489
no. of variables	667
R	0.025
R_w	0.038
GOF	1.80
max Δ/σ (final cycle)	0.21
residual density, e/Å^3	−0.41, +0.43 (both near Mo)

[a] Temperature 294 K, Enraf-Nonius CAD4-F diffractometer, Mo Kα radiation ($\lambda_{K\alpha_1}$ = 0.709 30, $\lambda_{K\alpha_2}$ = 0.713 59 Å), graphite monochromator, takeoff angle 2.7°, aperture (2.0 + tan θ) × 4.0 mm at a distance of 173 mm from the crystal, scan range extended by 25% on both sides for background measurement, $\sigma^2(I) = C + 2B + [0.04(C - B)]^2$ (S = scan rate, C = scan count, B = normalized background count), function minimized $\sum w(|F_o| - |F_c|)^2$, where $w = 4F_o^2/\sigma^2(F_o^2)$, $R = \sum||F_o| - |F_c||/\sum|F_o|$, $R_w = (\sum w(|F_o| - |F_c|)^2/\sum w|F_o|^2)^{1/2}$, and GOF = $[\sum(|F_o| - |F_c|)^2/(m - n)]^{1/2}$. Values given for R, R_w, and GOF are based on those reflections with $I \ge 3\sigma(I)$.

The structure analysis was initiated in the centrosymmetric space group $P\bar{1}$ on the basis of the Patterson function, this choice being confirmed by the subsequent successful solution and refinement of the structure. The solution was completed using conventional heavy-atom methods, the coordinates of the four molybdenum atoms (two from each of the two crystallographically independent molecules) being determined from the Patterson function and those of the remaining non-hydrogen atoms from a subsequent difference Fourier synthesis. Hydrogen atoms were fixed in idealized positions (C(sp^2)–H = 0.97 Å, C(sp^3)–H = 0.98 Å, $U_H = 1.2U_{bonded\ atom}$, methyl group orientations based on observed difference Fourier peaks). Neutral-atom scattering factors for all atoms and anomalous dispersion corrections for Mo and Si were taken from ref 21. Final atomic coordinates and

(17) Faller, J. W.; Ma, Y. *J. Organomet. Chem.* **1988**, *340*, 59. Data determined in this work are as follows. Anal. Calcd for $C_{20}H_{30}O_5Mo_2$: C, 44.29; H, 5.58. Found: C, 44.31; H, 5.67. IR (Nujol mull): $\nu_{Mo=O}$ 910 (s) and 878 (s) cm^{-1}; $\nu_{Mo-O-Mo}$ 762 (br) cm^{-1}. ^1H NMR (C_6D_6): δ 1.78 (s, $C_5(CH_3)_5$). Low-resolution mass spectrum (probe temperature 120 °C): m/z 526 [P^+ − O].

(18) Computer programs used include locally written programs for data processing and locally modified versions of the following: MULTAN80, multisolution program by P. Main, S. J. Fiske, S. E. Hull, L. Lessinger, G. Germain, J. P. Declercq, and M. M. Woolfson; ORFLS, full-matrix least squares, and ORFFE, functions and errors, by W. R. Busing, K. O. Martin, and H. A. Levy; FORDAP, Patterson and Fourier syntheses, by A. Zalkin; ORTEP II, illustrations, by C. K. Johnson.

(19) Coppens, P.; Leiserowitz, L.; Rabinovich, D. *Acta Crystallogr.* **1965**, *18*, 1035.

(20) Busing, W. R.; Levy, H. A. *Acta Crystallogr.* **1967**, *22*, 457.

(21) *International Tables for X-ray Crystallography*; Kynoch Press: Birmingham, England, 1974; Vol. IV, Tables 2.2B and 2.3.1.

Table V. Final Positional (Fractional ×10⁴, Mo and Si ×10⁵) and Isotropic Thermal Parameters ($U \times 10^3$ Å²) with Esd's in Parentheses for the Non-Hydrogen Atoms of Complex 2

atom	x	y	z	U_{eq}	atom	x	y	z	U_{eq}
Mo(1)	33420 (2)	31000 (1)	13487 (1)	35	C(20)	−915 (3)	416 (2)	1149 (2)	74
Mo(2)	5366 (2)	22313 (1)	10819 (1)	36	C(21)	4729 (2)	2230 (1)	1002 (1)	47
Mo(3)	22728 (2)	31796 (1)	63760 (1)	36	C(22)	5657 (3)	433 (2)	983 (2)	72
Mo(4)	53657 (2)	23441 (1)	60789 (1)	36	C(23)	3753 (3)	862 (2)	2045 (2)	76
Si(1)	50302 (6)	12432 (4)	15857 (4)	50	C(24)	6079 (3)	1399 (2)	2313 (2)	79
Si(2)	681 (6)	22660 (5)	29459 (4)	46	C(25)	246 (3)	1614 (2)	2158 (1)	59
Si(3)	11915 (7)	13139 (5)	67347 (6)	53	C(26)	674 (3)	1660 (2)	3802 (2)	80
Si(4)	58585 (6)	24242 (5)	79334 (4)	49	C(27)	−1487 (3)	2542 (3)	3078 (2)	83
O(1)	1968 (1)	2634 (1)	1187 (1)	41	C(28)	727 (3)	3243 (2)	2837 (2)	73
O(2)	3817 (2)	2782 (2)	2953 (1)	91	C(29)	2570 (3)	4518 (2)	5876 (2)	67
O(3)	−1251 (2)	3651 (1)	1182 (2)	87	C(30)	2023 (3)	4198 (2)	5302 (2)	58
O(4)	3812 (1)	2730 (1)	6236 (1)	40	C(31)	922 (2)	4052 (1)	5540 (2)	49
O(5)	1873 (3)	2989 (2)	7981 (1)	96	C(32)	784 (2)	4269 (2)	6270 (2)	57
O(6)	6732 (2)	3759 (1)	6079 (2)	93	C(33)	1827 (3)	4563 (2)	6482 (2)	68
N(1)	3596 (2)	2817 91)	2296 (1)	50	C(34)	3753 (4)	4797 (2)	5843 (4)	127
N(2)	−458 (2)	3096 (1)	1200 (1)	54	C(35)	2508 (4)	4092 (3)	4539 (2)	104
N(3)	2101 (2)	2967 (1)	7333 (1)	53	C(36)	9 (3)	3801 (2)	5062 (2)	76
N(4)	6102 (2)	3213 (1)	6142 (1)	55	C(37)	−272 (3)	4254 (3)	6733 (2)	94
C(1)	2578 (3)	4459 (2)	931 (2)	69	C(38)	2042 (5)	4937 (2)	7194 (3)	120
C(2)	3215 (3)	4179 (2)	324 (2)	59	C(39)	6774 (2)	1775 (2)	5281 (1)	51
C(3)	4369 (2)	4036 (1)	547 (1)	48	C(40)	5776 (2)	2147 (2)	4869 (1)	48
C(4)	4454 (2)	4203 (2)	1291 (2)	53	C(41)	4877 (2)	1650 (2)	5042 (1)	46
C(5)	3320 (3)	4474 (2)	1535 (2)	64	C(42)	5291 (2)	1010 (1)	5576 (1)	47
C(6)	1301 (3)	4710 (2)	921 (3)	122	C(43)	6469 (2)	1084 (2)	5718 (1)	49
C(7)	2750 (4)	4112 (3)	−437 (2)	106	C(44)	7944 (3)	2051 (2)	5219 (2)	76
C(8)	5355 (3)	3836 (2)	50 (2)	76	C(45)	5751 (3)	2857 (2)	4291 (2)	66
C(9)	5530 (3)	4162 (2)	1746 (2)	87	C(46)	3704 (3)	1781 (2)	4695 (2)	63
C(10)	3027 (5)	4780 (2)	2281 (3)	112	C(47)	4650 (3)	330 (2)	5919 (2)	71
C(11)	−775 (2)	1753 (2)	289 (1)	48	C(48)	7275 (3)	449 (2)	6165 (2)	73
C(12)	119 (2)	2091 (2)	−128 (1)	47	C(49)	1207 (2)	2257 (2)	6090 (2)	53
C(13)	1148 (2)	1543 (2)	13 (1)	50	C(50)	988 (4)	428 (2)	6188 (3)	126
C(14)	906 (2)	898 (2)	524 (1)	51	C(51)	−60 (4)	1520 (3)	7351 (3)	117
C(15)	−285 (2)	1027 (2)	696 (1)	50	C(52)	2490 (3)	1026 (2)	7329 (2)	80
C(16)	−2013 (2)	2087 (2)	265 (2)	70	C(53)	5959 (3)	1762 (2)	7149 (1)	58
C(17)	−41 (3)	2845 (2)	−669 (2)	64	C(54)	5439 (4)	1778 (2)	8777 (2)	98
C(18)	2276 (3)	1647 (2)	−349 (2)	70	C(55)	7287 (3)	2751 (3)	8095 (2)	91
C(19)	1694 (3)	147 (2)	796 (2)	81	C(56)	4855 (3)	3391 (2)	7814 (2)	78

equivalent isotropic thermal parameters ($U_{eq} = {}^1/_3$(trace diagonalized U)) for **2** are given in Table V. Selected bond lengths (Å) and bond angles (deg) for the compound are listed in Tables VI and VII, respectively. Anisotropic thermal parameters, torsion angles, calculated hydrogen atom coordinates, and the remaining molecular dimensions for **2** are provided as supplementary material. A stereoview of the solid-state molecular structure of both independent molecules of $[Cp^*Mo(NO)(CH_2SiMe_3)]_2(\mu\text{-}O)$ is displayed in Figure 2.

Results and Discussion

Syntheses. This portion of our report begins with the comparison of two reactions which, at first glance, would be expected to be quite similar. Previous work in these laboratories[12,22] has established that the preparation of the tungsten dialkyl complexes $Cp'W(NO)(CH_2SiMe_3)_2$ is straightforward via reaction of $Cp'W(NO)I_2$ with 2 equiv of a (trimethylsilyl)methyl Grignard reagent followed by hydrolysis with water, i.e.

$$Cp'W(NO)I_2 \xrightarrow[(2)\ H_2O\ (excess)]{(1)\ 2Me_3SiCH_2MgCl} Cp'W(NO)(CH_2SiMe_3)_2 \quad (1)$$

Conversion 1 consistently affords the $Cp'W(NO)(CH_2SiMe_3)_2$ complexes in 80% isolated yields. We have now discovered that the similar reaction involving one of the congeneric molybdenum diiodide starting materials is not as straightforward as for the case of tungsten. Thus, treating $Cp^*Mo(NO)I_2$ with 2 equiv of an ethereal solution of Me_3SiCH_2MgCl followed by quenching with water leads to the formation of three isolable organometallic products, the *minor* one being the expected $Cp^*Mo(NO)(CH_2SiMe_3)_2$, i.e.

$$Cp^*Mo(NO)I_2 \xrightarrow[(2)\ H_2O\ (excess)]{(1)\ 2Me_3SiCH_2MgCl} \underset{\mathbf{1}\ (2\%)}{Cp^*Mo(NO)(CH_2SiMe_3)_2} + \underset{\mathbf{2}\ (8\%)}{[Cp^*Mo(NO)(CH_2SiMe_3)]_2(\mu\text{-}O)} + \underset{\mathbf{3}\ (27\%)}{[Cp^*Mo(NO)I]_2} \quad (2)$$

Hence, the desired dialkyl complex, **1**, is indeed among the final isolated products but in abysmal yield. Complex **3** presumably results via the loss of iodide from the $[Cp^*Mo(NO)I_2]^{\bullet-}$ radical anion, which is the first intermediate formed in metathesis reactions of this type.[23] However, the key point to emerge from reaction 2 is that, unlike its tungsten congener, $Cp^*Mo(NO)(CH_2SiMe_3)_2$ is unstable with respect to hydrolysis. We were sufficiently intrigued by this observation to expend some effort to gain some insight into how complex **2** is formed and whether this type of reactivity is generally characteristic of such $Cp'Mo(NO)R_2$ (R = alkyl, aryl) compounds. The rest of this paper presents the results of those investigations, as well as a comparison of the reactivity of dialkyl and diaryl complexes of both molybdenum and tungsten with water.

In order to perform some of the investigations referred to in the preceding paragraph, we required clean preparative routes to each of the complexes **1**–**3** isolated initially from reaction 2. We have subsequently discovered that they can indeed be individually synthesized in good yields

(22) Martin, J. T. Ph.D. Dissertation, The University of British Columbia, 1987.

(23) Herring, F. G.; Legzdins, P.; Richter-Addo, G. B. *Organometallics* 1989, *8*, 1485.

Table VI. Bond Lengths (Å) with Esd's in Parentheses for Complex 2

Mo(1)–O(1)	1.9001 (15)	Si(4)–C(53)	1.861 (3)
Mo(1)–N(1)	1.758 (2)	Si(4)–C(54)	1.882 (4)
Mo(1)–C(1)	2.361 (3)	Si(4)–C(55)	1.854 (4)
Mo(1)–C(2)	2.443 (3)	Si(4)–C(56)	1.860 (3)
Mo(1)–C(3)	2.443 (2)	O(2)–N(1)	1.218 (3)
Mo(1)–C(4)	2.345 (2)	O(3)–N(2)	1.224 (3)
Mo(1)–C(5)	2.302 (3)	O(5)–N(3)	1.209 (3)
Mo(1)–C(21)	2.170 (2)	O(6)–N(4)	1.224 (3)
Mo(1)–Cp(1)	2.0528 (12)	C(1)–C(2)	1.413 (5)
Mo(2)–O(1)	1.8945 (15)	C(1)–C(5)	1.405 (5)
Mo(2)–N(2)	1.758 (2)	C(1)–C(6)	1.512 (5)
Mo(2)–C(11)	2.357 (2)	C(2)–C(3)	1.406 (4)
Mo(2)–C(12)	2.290 (2)	C(2)–C(7)	1.503 (5)
Mo(2)–C(13)	2.399 (2)	C(3)–C(4)	1.408 (4)
Mo(2)–C(14)	2.480 (2)	C(3)–C(8)	1.494 (4)
Mo(2)–C(15)	2.450 (2)	C(4)–C(5)	1.439 (4)
Mo(2)–C(25)	2.165 (3)	C(4)–C(9)	1.505 (5)
Mo(2)–Cp(2)	2.0695 (12)	C(5)–C(10)	1.512 (5)
Mo(3)–O(4)	1.9013 (15)	C(11)–C(12)	1.430 (3)
Mo(3)–N(3)	1.758 (2)	C(11)–C(15)	1.406 (4)
Mo(3)–C(29)	2.362 (3)	C(11)–C(16)	1.496 (4)
Mo(3)–C(30)	2.446 (2)	C(12)–C(13)	1.431 (4)
Mo(3)–C(31)	2.444 (2)	C(12)–C(17)	1.503 (4)
Mo(3)–C(32)	2.346 (2)	C(13)–C(14)	1.398 (4)
Mo(3)–C(33)	2.290 (3)	C(13)–C(18)	1.503 (4)
Mo(3)–C(49)	2.169 (3)	C(14)–C(15)	1.432 (4)
Mo(3)–Cp(3)	2.0539 (12)	C(14)–C(19)	1.499 (4)
Mo(4)–O(4)	1.8946 (15)	C(15)–C(20)	1.501 (4)
Mo(4)–N(4)	1.761 (2)	C(29)–C(30)	1.397 (5)
Mo(4)–C(39)	2.366 (2)	C(29)–C(33)	1.407 (5)
Mo(4)–C(40)	2.292 (2)	C(29)–C(34)	1.513 (5)
Mo(4)–C(41)	2.388 (2)	C(30)–C(31)	1.405 (4)
Mo(4)–C(42)	2.451 (2)	C(30)–C(35)	1.516 (5)
Mo(4)–C(43)	2.448 (2)	C(31)–C(32)	1.407 (4)
Mo(4)–C(53)	2.166 (3)	C(31)–C(36)	1.498 (4)
Mo(4)–Cp(4)	2.0610 (12)	C(32)–C(33)	1.434 (4)
Si(1)–C(21)	1.852 (3)	C(32)–C(37)	1.503 (5)
Si(1)–C(22)	1.879 (3)	C(33)–C(38)	1.513 (5)
Si(1)–C(23)	1.863 (3)	C(39)–C(40)	1.438 (4)
Si(1)–C(24)	1.862 (3)	C(39)–C(43)	1.406 (4)
Si(2)–C(25)	1.858 (3)	C(39)–C(44)	1.499 (4)
Si(2)–C(26)	1.864 (3)	C(40)–C(41)	1.427 (4)
Si(2)–C(27)	1.854 (3)	C(40)–C(45)	1.495 (4)
Si(2)–C(28)	1.852 (3)	C(41)–C(42)	1.407 (4)
Si(3)–C(49)	1.856 (3)	C(41)–C(46)	1.502 (4)
Si(3)–C(50)	1.867 (5)	C(42)–C(43)	1.431 (4)
Si(3)–C(51)	1.868 (4)	C(42)–C(47)	1.507 (4)
Si(3)–C(52)	1.863 (4)	C(43)–C(48)	1.504 (4)

simply by changing the starting material or the reaction conditions.

The isolated yield of Cp*Mo(NO)(CH_2SiMe_3)$_2$ (1) using Cp*Mo(NO)Cl_2 (eq 3) as starting material is about 30 times greater (i.e. 60% vs 2%) than when Cp*Mo(NO)I_2 is employed as the initial reactant. This fact reflects both the

$$\text{Cp*Mo(NO)Cl}_2 \xrightarrow{2\text{Me}_3\text{SiCH}_2\text{MgCl}} \mathbf{1}\ (60\%) \qquad (3)$$

relative stabilities of the radical anion intemediates produced during the metathesis reactions[23] and the ease of workup of the final reaction mixtures. It is also important that no water be used during the isolation of this organometallic compound.[24]

[Cp*Mo(NO)(CH_2SiMe_3)]$_2$(μ-O) (2) is best synthesized (eq 4) by generating 1 in Et_2O, treating it with water, and then chromatographing the final mixture on alumina III or Florisil with Et_2O as eluant.

$$\text{Cp*Mo(NO)Cl}_2 \xrightarrow[(2)\ \text{H}_2\text{O (excess)}]{(1)\ 2\text{Me}_3\text{SiCH}_2\text{MgCl}} \mathbf{2}\ (75\%) \qquad (4)$$

(CH_2SiMe_3)]$_2$(μ-O) can also be obtained by treatment of isolated Cp*Mo(NO)(CH_2SiMe_3)$_2$ with water in benzene or THF (eq 5). Clearly, the transformation from 1 and 2 is clean and chemically straightforward (eq 5).

$$\mathbf{1} \xrightarrow{\text{H}_2\text{O}} \mathbf{2}\ (95\%\ \text{by}\ ^1\text{H NMR spectroscopy}) \qquad (5)$$

Finally, the reduction product of reaction 2, [Cp*Mo(NO)I]$_2$ (3), is most conveniently synthesized by treatment of Cp*Mo(NO)I_2 with zinc amalgam in THF (eq 6).

Table VII. Bond Angles (deg) with Esd's in Parentheses for Complex 2

O(1)–Mo(1)–N(1)	101.75 (9)	C(3)–C(2)–C(7)	126.5 (3)
O(1)–Mo(1)–C(21)	106.45 (8)	C(2)–C(3)–C(4)	108.9 (2)
O(1)–Mo(1)–Cp(1)	122.31 (6)	C(2)–C(3)–C(8)	125.2 (3)
N(1)–Mo(1)–C(21)	93.93 (10)	C(4)–C(3)–C(8)	125.6 (3)
N(1)–Mo(1)–Cp(1)	119.00 (8)	C(3)–C(4)–C(5)	107.6 (3)
C(21)–Mo(1)–Cp(1)	109.27 (8)	C(3)–C(4)–C(9)	127.0 (3)
O(1)–Mo(2)–N(2)	103.47 (9)	C(5)–C(4)–C(9)	125.3 (3)
O(1)–Mo(2)–C(25)	104.05 (10)	C(1)–C(5)–C(4)	106.8 (3)
O(1)–Mo(2)–Cp(2)	122.59 (6)	C(1)–C(5)–C(10)	127.7 (3)
N(2)–Mo(2)–C(25)	94.64 (11)	C(4)–C(5)–C(10)	125.4 (4)
N(2)–Mo(2)–Cp(2)	118.88 (8)	C(12)–C(11)–C(15)	107.4 (2)
C(25)–Mo(2)–Cp(2)	108.80 (8)	C(12)–C(11)–C(16)	126.2 (3)
O(4)–Mo(3)–N(3)	102.32 (9)	C(15)–C(11)–C(16)	126.3 (3)
O(4)–Mo(3)–C(49)	106.52 (9)	C(11)–C(12)–C(13)	107.8 (2)
O(4)–Mo(3)–Cp(3)	121.87 (6)	C(11)–C(12)–C(17)	125.1 (2)
N(3)–Mo(3)–C(49)	93.81 (11)	C(13)–C(12)–C(17)	126.9 (2)
N(3)–Mo(3)–Cp(3)	118.41 (9)	C(12)–C(13)–C(14)	108.2 (2)
C(49)–Mo(3)–Cp(3)	109.89 (8)	C(12)–C(13)–C(18)	124.8 (3)
O(4)–Mo(4)–N(4)	104.72 (9)	C(14)–C(13)–C(18)	126.9 (3)
O(4)–Mo(4)–C(53)	103.99 (9)	C(13)–C(14)–C(15)	108.0 (2)
O(4)–Mo(4)–Cp(4)	121.65 (6)	C(13)–C(14)–C(19)	127.5 (3)
N(4)–Mo(4)–C(53)	94.12 (11)	C(15)–C(14)–C(19)	124.3 (3)
N(4)–Mo(4)–Cp(4)	119.80 (8)	C(11)–C(15)–C(14)	108.6 (2)
C(53)–Mo(4)–Cp(4)	108.02 (8)	C(11)–C(15)–C(20)	126.4 (3)
C(21)–Si(1)–C(22)	108.18 (14)	C(14)–C(15)–C(20)	124.5 (3)
C(21)–Si(1)–C(23)	114.63 (14)	Mo(1)–C(21)–Si(1)	116.72 (13)
C(21)–Si(1)–C(24)	107.61 (14)	Mo(2)–C(25)–Si(2)	117.02 (14)
C(22)–Si(1)–C(23)	107.5 (2)	C(30)–C(29)–C(33)	108.7 (3)
C(22)–Si(1)–C(24)	110.4 (2)	C(30)–C(29)–C(34)	125.7 (4)
C(23)–Si(1)–C(24)	108.5 (2)	C(33)–C(29)–C(34)	125.6 (4)
C(25)–Si(2)–C(26)	109.42 (15)	C(29)–C(30)–C(31)	108.1 (3)
C(25)–Si(2)–C(27)	107.7 (2)	C(29)–C(30)–C(35)	125.4 (3)
C(25)–Si(2)–C(28)	115.91 (13)	C(31)–C(30)–C(35)	126.4 (3)
C(26)–Si(2)–C(27)	108.5 (2)	C(30)–C(31)–C(32)	108.7 (3)
C(26)–Si(2)–C(28)	107.9 (2)	C(30)–C(31)–C(36)	125.1 (3)
C(27)–Si(2)–C(28)	107.2 (2)	C(32)–C(31)–C(36)	125.9 (3)
C(49)–Si(3)–C(50)	108.7 (2)	C(31)–C(32)–C(33)	107.1 (3)
C(49)–Si(3)–C(51)	106.1 (2)	C(31)–C(32)–C(37)	127.3 (3)
C(49)–Si(3)–C(52)	115.70 (14)	C(33)–C(32)–C(37)	125.5 (3)
C(50)–Si(3)–C(51)	109.9 (3)	C(29)–C(33)–C(32)	107.4 (3)
C(50)–Si(3)–C(52)	108.4 (2)	C(29)–C(33)–C(38)	126.1 (4)
C(51)–Si(3)–C(52)	108.0 (2)	C(32)–C(33)–C(38)	126.1 (4)
C(53)–Si(4)–C(54)	107.60 (15)	C(40)–C(39)–C(43)	107.7 (2)
C(53)–Si(4)–C(55)	108.6 (2)	C(40)–C(39)–C(44)	125.8 (3)
C(53)–Si(4)–C(56)	116.72 (13)	C(43)–C(39)–C(44)	126.4 (3)
C(54)–Si(4)–C(55)	109.1 (2)	C(39)–C(40)–C(41)	107.6 (2)
C(54)–Si(4)–C(56)	108.9 (2)	C(39)–C(40)–C(45)	125.1 (2)
C(55)–Si(4)–C(56)	105.8 (2)	C(41)–C(40)–C(45)	126.8 (2)
Mo(1)–O(1)–Mo(2)	175.12 (9)	C(40)–C(41)–C(42)	108.1 (2)
Mo(3)–O(4)–Mo(4)	176.74 (9)	C(40)–C(41)–C(46)	125.5 (3)
Mo(1)–N(1)–O(2)	167.0 (2)	C(42)–C(41)–C(46)	126.4 (3)
Mo(2)–N(2)–O(3)	168.8 (2)	C(41)–C(42)–C(43)	108.1 (2)
Mo(3)–N(3)–O(5)	166.3 (2)	C(41)–C(42)–C(47)	127.1 (3)
Mo(4)–N(4)–O(6)	167.9 (2)	C(43)–C(42)–C(47)	124.7 (3)
C(2)–C(1)–C(5)	109.3 (3)	C(39)–C(43)–C(42)	108.4 (2)
C(2)–C(1)–C(6)	124.7 (4)	C(39)–C(43)–C(48)	126.1 (3)
C(5)–C(1)–C(6)	125.9 (4)	C(42)–C(43)–C(48)	124.9 (3)
C(1)–C(2)–C(3)	107.3 (3)	Mo(3)–C(49)–Si(3)	117.97 (14)
C(1)–C(2)–C(7)	126.0 (3)	Mo(4)–C(53)–Si(4)	116.82 (13)

(24) Many reactions of Cp'M(NO)X_2 compounds (X = halide) with Grignard reagents, RMgX, result in the formation of [Cp'M(NO)R_2]$_2$MgX$_2$·solvent complexes which upon treatment with water liberate Cp'M(NO)R_2. These intermediate complexes are recognizable as brown to red insoluble precipitates in the final reaction mixtures. The small amount of the [Cp*Mo(NO)(CH_2SiMe_3)$_2$]$_2$·$MgCl_2$·Et_2O complex formed during the reaction is best discarded. See ref 12 for descriptions of the partial crystal structures of [CpM(NO)(CH_2SiMe_3)$_2$]$_2$$MgI_2$·$Et_2O$ (M = Mo, W).

$$Cp^*Mo(NO)I_2 \xrightarrow{0.5Zn/Hg} \mathbf{3}\ (34\%) \qquad (6)$$

The conversion portrayed in eq 4 is just one example of a much more general phenomenon. Thus, the transformations of $Cp'Mo(NO)Cl_2$ to $[Cp'Mo(NO)R]_2(\mu\text{-}O)$ (R = alkyl, aryl) via $Cp'Mo(NO)R_2$ appear to be ubiquitous (eq 7). As indicated in eq 7, both RMgX and R_2Mg reagents may be used to generate the requisite $Cp'Mo(NO)R_2$ species in situ. Subsequent hydrolysis then affords a variety of bimetallic analogues of **2** whose physical properties are collected in Tables I–III. Several features of these otherwise straightforward conversions (7) merit some comment. For instance, the (trimethylsilyl)methyl derivatives (i.e. complexes **2** and **4**) are consumed by water over a period of about 5 min in Et_2O at ambient temperatures. However, $Cp^*Mo(NO)(CH_2CMe_3)_2$ takes several hours at 20 °C to decompose to **5** in THF even in the presence of 30 equiv of water. The aryl-containing complexes $[Cp^*Mo(NO)R]_2(\mu\text{-}O)$ (R = *o*-tolyl (**7**), Ph (**8**)) are best synthesized by adding water to THF solutions of in situ generated $Cp^*Mo(NO)(aryl)_2$ since the latter species are extremely air- and moisture-sensitive.[13a] Indeed, our attempts to synthesize the Cp analogues of **7** and **8** have been thwarted by the instability of the precursor $CpMo(NO)(aryl)_2$ complexes.

$$Cp'Mo(NO)Cl_2 \xrightarrow[\text{or } R_2Mg]{2RMgX} Cp'Mo(NO)R_2 \xrightarrow[-2RH]{H_2O} \tfrac{1}{2}[Cp'Mo(NO)R]_2(\mu\text{-}O) \qquad (7)$$

R = alkyl, aryl

These new $[Cp'Mo(NO)R]_2(\mu\text{-}O)$ (R = alkyl, aryl) bimetallic complexes are moderately air-stable as solids, but in solution they are generally air-sensitive and decompose eventually to the $[Cp'Mo(O)_2]_2(\mu\text{-}O)$ compounds.[17] This latter result has been established specifically for complexes **2**, **5**, and **8**. In contrast, complex **7** is sufficiently air-stable to be crystallized in air by slow evaporation of solvent. Perhaps the steric bulk of the *o*-methyl group in **7** provides enough protection for the metal to shield it from attack by water or oxygen. The alkyl derivatives (i.e. complexes **2** and **4**–**6**) are dark red-brown to red-black crystalline solids which generally exhibit high thermal stability. For instance, thermolysis of a sample of **2** in benzene in an NMR tube at 80 °C for 2 days results in no detectable change in the NMR spectrum of the sample. The aryl derivatives are chocolate brown and tend to be less crystalline than their alkyl congeners. The mass spectral, elemental analysis, and IR and NMR data for complexes **1**–**8** are collected in Tables I–III.

Spectroscopic and Physical Properties of $[Cp^*Mo(NO)(CH_2SiMe_3)]_2(\mu\text{-}O)$ (2). Since **2** is the prototypal complex in this family, its properties will be considered in some detail. The 300-MHz ^1H NMR spectrum of $[Cp^*Mo(NO)(CH_2SiMe_3)]_2(\mu\text{-}O)$ in C_6D_6 (Figure 1) exhibits an AB pattern at 0.84 and 0.75 ppm (J_{AB} = 12.3 Hz) for the two pairs of diastereotopic methylene protons and singlet resonances at 1.59 and 0.45 ppm due to the methyl protons of the Cp* ligands and the methyl groups attached to the silicon atoms, respectively. In comparison, the two pairs of diastereotopic methylene protons in **1** give rise to an AX doublet of doublets at 2.21 and −1.17 ppm (J_{AX} = 10.8 Hz) while the Cp* and $SiMe_3$ protons resonate at 1.49 and 0.37 ppm, respectively (Table III). The principal feature that differentiates the two spectra is the existence of two small singlets at 1.71 and 0.42 ppm evident in Figure 1. These latter resonances can be assigned to the Cp* and $SiMe_3$ protons, respectively, of a minor isomer of **2**. Signals due to the methylene protons of the minor isomer are not, however, observable. The isomers are probably diastereomers, since they do not interconvert (vide supra), and have thus been assigned the molecular structures shown in Figure 1. The solid-state molecular structure of $[Cp^*Mo(NO)(CH_2SiMe_3)]_2(\mu\text{-}O)$ (Figure 2) reveals it to be the *S,R* isomer with the two chiral $[Cp^*Mo(NO)(CH_2SiMe_3)]$ units being twisted by 90° with respect to each other about the Mo–O–Mo bond. The other diastereomer probably has the same relative configurations at the metal centers, i.e. *R,R* or *S,S*, the latter isomer being shown in Figure 1. The *S,R* isomer is probably the dominant form in solution, as molecular models show that the *S,S* isomer possesses severe steric interactions between the methyl groups of the Cp* ligand on one molybdenum with the bulky CH_2SiMe_3 group on the other Mo center. The existence of these isomers is also evident in the $^{13}C\{^1H\}$ NMR spectrum of $[Cp^*Mo(NO)(CH_2SiMe_3)]_2(\mu\text{-}O)$ (Table III). Consistent with the view that steric factors control the ratio of the two isomers is the fact that for $[Cp^*Mo(NO)(CH_2SiMe_3)]_2(\mu\text{-}O)$ the ratio major:minor = 9:1 while the less sterically encumbered $[CpMo(NO)(CH_2SiMe_3)]_2(\mu\text{-}O)$ exhibits an isomer ratio of major:minor = 3:1. As summarized in Table III, where the major and minor isomers are designated as A and B, respectively, the ratios of similar $[Cp'Mo(NO)R]_2(\mu\text{-}O)$ isomers are generally dependent on the steric bulk of the Cp′ ligand as well as that of the alkyl or aryl ligand.

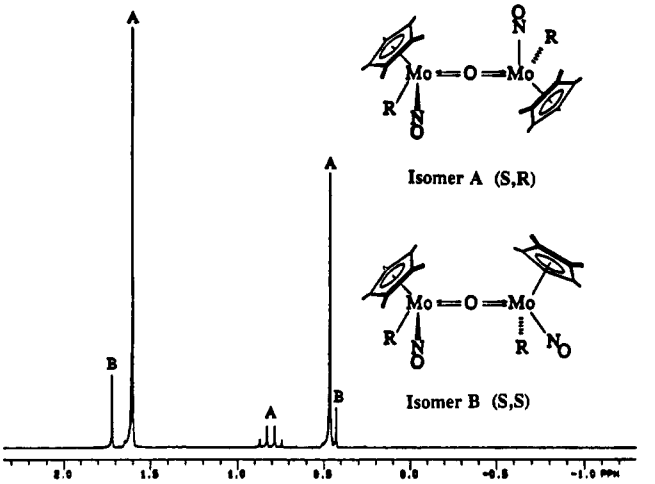

Figure 1. ^1H NMR spectrum of **2** in C_6D_6 (300 MHz).

The IR spectral features exhibited by these bimetallic μ-oxo complexes (Table II) are different from those displayed by their parent bis(hydrocarbyl) complexes $Cp'Mo(NO)R_2$. The IR spectra of $[Cp'Mo(NO)R]_2(\mu\text{-}O)$ exhibit strong bands in the region 820–740 cm^{-1} which are diagnostic of Mo–O–Mo vibrations.[25] The nitrosyl stretching frequencies of these bimetallic complexes are some 10–50 cm^{-1} lower in energy than the ν_{NO} bands exhibited by their parent bis(hydrocarbyl) complexes. This spectral feature is indicative of there being more electron density available on the molybdenum centers for backbonding into the antibonding orbitals of the nitrosyl ligand in these μ-oxo complexes than in their parent dialkyl and diaryl complexes. Therefore, this would suggest that the bridging oxo ligand is providing each molybdenum center with one electron in the σ Mo–O link and some electron density associated with the lone pairs of electrons in its p orbitals. This view is in accord with the X-ray crystallographic results discussed in the next section.

(25) Barraclough, C. G.; Lewis, J.; Nyholm, R. S. *J. Chem. Soc.* **1959**, 3552.

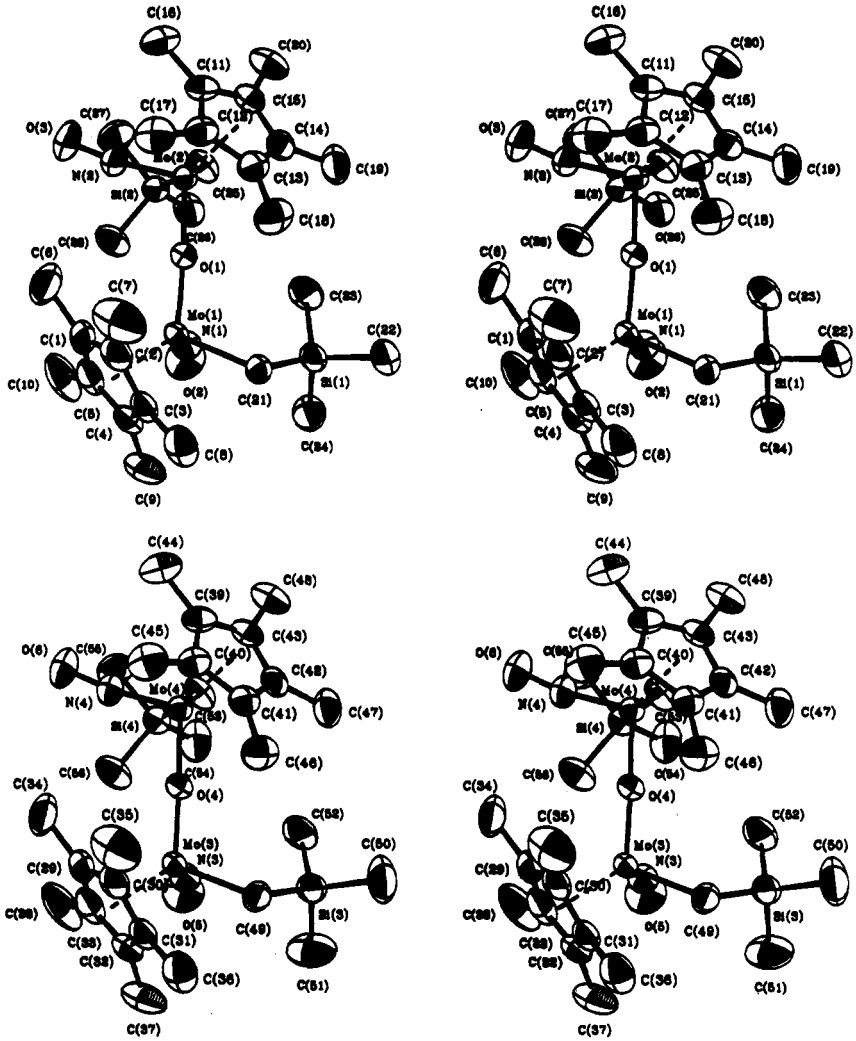

Figure 2. Stereoviews of the two crystallographically independent molecules of **2**. Thermal ellipsoids of 50% probability are shown for the non-hydrogen atoms.

Solid-State Molecular Structure of 2. A single-crystal X-ray crystallographic analysis of [Cp*Mo(NO)-(CH_2SiMe_3)]$_2$(μ-O) has confirmed its bimetallic nature and has established the *S,R* configurations at the metal centers. ORTEP diagrams of complex **2** are presented in Figure 2. The pertinent crystallographic and experimental data are contained in Table IV, and selected bond lengths and bond angles of both independent molecules in the asymmetric unit are presented in Tables VI and VII, respectively. Each crystallographically independent molecule has a three-legged piano-stool molecular geometry (pseudooctahedral) about each molybdenum center. At each center (e.g. Mo(1)) the nitrosyl ligand is bonded in an essentially linear fashion (Mo(1)–N(1)–O(2) = 167.0 (2)°). The short Mo–N (Mo(1)–N(1) = 1.758 (2) Å) and long N–O (N(1)–O(2) = 1.218 (3) Å) bond lengths suggest that there is considerable Mo→NO back-bonding extant in the molecule.[26] The most chemically interesting feature of the structure involves the orientation of the two {Cp*Mo(NO)(CH_2SiMe_3)} units with respect to each other about the Mo–O–Mo linkage. The oxo bridge between the two molybdenum centers is essentially linear (e.g. Mo(1)–O(1)–Mo(2) = 175.12 (9)°), and the two {Cp*Mo(NO)(CH_2SiMe_3)} units are twisted by approximately 90° with respect to one another (e.g. N(1)–Mo(1)–Mo(2)–N(2) = 94°). This intramolecular dimension, taken together with the short Mo–O bond lengths (e.g. Mo(1)–O(1) = 1.9001 (15) Å and Mo(2)–O(1) = 1.8945 (15) Å), which are intermediate between typical Mo—O and Mo=O bond lengths,[27] suggests that there is a considerable degree of multiple bonding in the central Mo–O–Mo linkage of the bimetallic complex. If the Mo–O–Mo axis is defined as the *z* axis, the Mo=O=Mo π interaction involves overlap between an empty d orbital on each of the {Cp*Mo(NO)(CH_2SiMe_3)} groups with the appropriate filled p orbital (i.e. p_x for one group and p_y for the one orthogonal to it) on the bridging oxygen atom. This localized view of the π bonding in the Mo=O=Mo bridge suggests that each Mo center thus achieves the favored 18-valence-electron configuration.[28]

The intramolecular dimensions of the Mo–O–Mo bridging unit in [Cp*Mo(NO)(CH_2SiMe_3)]$_2$(μ-O) (**2**) may be compared to those reported for other oxo-bridged complexes. The Mo–O–Mo angle in the crystallographi-

(26) Feltham, R. D.; Enemark, J. H. In *Topics in Inorganic and Organometallic Stereochemistry*; Geoffroy, G. L., Ed.; Wiley-Interscience: New York, 1981; Chapter 4.

(27) Orpen, A. G.; Brammer, L.; Allen, F. H.; Kennard, O.; Watson, D. G.; Taylor, R. *J. Chem. Soc., Dalton Trans.* **1989**, S1.

(28) In these complexes the bridging oxo ligand may be regarded as a formal 6-electron donor, three electrons being donated to each Mo center so that the metal can reach electronic saturation. The metal centers in these bimetallic complexes thus resemble those in the monomeric 18-electron alkoxide complexes Cp'Mo(NO)(R)(OR) (R = alkyl),[29] in which the alkoxide groups also function as 3-electron donors to the 15-electron Cp'Mo(NO)(R) fragments.

(29) Legzdins, P.; Lundmark, P. J.; Rettig, S. J., manuscript in preparation.

Table VIII. Data for the First Electrochemical Reductions of Complexes 1 and 2[a]

scan rate, V s^{-1}	$E^{\circ\prime}_1$,[b] V	ΔE,[c] V	$i_{p,a}/i_{p,c}$[d]
	Complex 1		
0.80	−1.52	0.69 (0.20)	1.0
0.60	−1.55	0.47 (0.18)	1.0
0.40	−1.54	0.49 (0.15)	1.0
0.20	−1.56	0.36 (0.12)	1.0
0.10	−1.59	0.28 (0.10)	0.9
	Complex 2		
0.80	−1.37	0.19 (0.18)	1.0
0.60	−1.38	0.17 (0.16)	1.0
0.40	−1.38	0.15 (0.14)	1.0
0.20	−1.39	0.12 (0.11)	1.0
0.10	−1.37	0.09 (0.09)	1.0

[a] In THF containing 0.10 M $[n\text{-Bu}_4N]PF_6$, at a Pt-bead working electrode. Potentials are measured vs Ag wire. [b] Defined as the average of the cathodic and anodic peak potentials (±0.02 V). [c] Defined as the separation of the cathodic and anodic peak potentials. Values of ΔE given in parentheses are for the Cp_2Fe/Cp_2Fe^+ couple under the same conditions. [d] Ratio of anodic peak current to cathodic peak current.

cally characterized complex $[Cp^*Mo(O)_2]_2(\mu\text{-O})$ is 178° and the M–O bond lengths are ~1.86 Å.[17] Similarly, the linear (180°) Mo–O–Mo bridge in $[(HB(pz)_3)Mo(O)Cl]_2(\mu\text{-O})$ exhibits Mo–O bond lengths of 1.861 (1) Å.[30] Both of these examples show oxo ligands that are quite similar to that existing in **2**. In contrast, $[Ir(PPh_3)(NO)]_2(\mu\text{-O})$ (the only other oxo-bridged nitrosyl complex that has been structurally characterized) exhibits an acute Ir–O–Ir angle of 82.3 (3)°, long Ir–O bond lengths of ~1.94 Å, and an Ir–Ir separation of 2.55 Å.[31] The $Ir(PPh_3)(NO)$ fragment, like $Cp^*Mo(NO)R$, is formally a 14-electron species. However, rather than engaging in multiple Ir=O=Ir bonding to attain diamagnetism, the later transition metal (being a softer Lewis acid than Mo) evidently prefers to form a direct Ir–Ir bond.

Electrochemical Studies. During previous investigations, we have found knowledge of the fundamental redox properties of organometallic complexes to be a useful guide in directing our studies of their characteristic chemical properties.[23] It was therefore of interest to us to determine the electrochemical behavior of complexes **1** and **2** as representative examples of their particular classes of compounds. The electrochemical data for both complexes are compiled in Table VIII.

The cyclic voltammogram of complex **1** in THF (Figure 3a) reveals that it undergoes a quasi-reversible, one-electron reduction at approximately $E^{\circ\prime} = -1.55$ V vs Ag wire. While the $i_{p,a}/i_{p,c}$ ratio for this feature indicates reversibility, it is clear from the ΔE values (Table VIII) that electron transfer in this system occurs at a slower rate than for the ferrocene standard. Nevertheless, the reduction potential of **1** is comparable to that exhibited by the related tungsten dialkyl complex $Cp^*W(NO)(CH_2CMe_2Ph)_2$, for which $E^{\circ\prime} = -1.62$ V.[1] Interestingly, no second reduction of **1** occurs out to the solvent limit, even though the dianion $[Cp^*Mo(NO)(CH_2SiMe_3)_2]^{2-}$ should exist.[1,32]

The cyclic voltammogram of complex **2** in THF (Figure 3c) indicates that the compound undergoes a reversible, one-electron reduction and a second, irreversible, one-electron reduction at the more negative potential $E_{p,c} = -2.18$ V. The first reduction potential for **2** (Figure 3b)

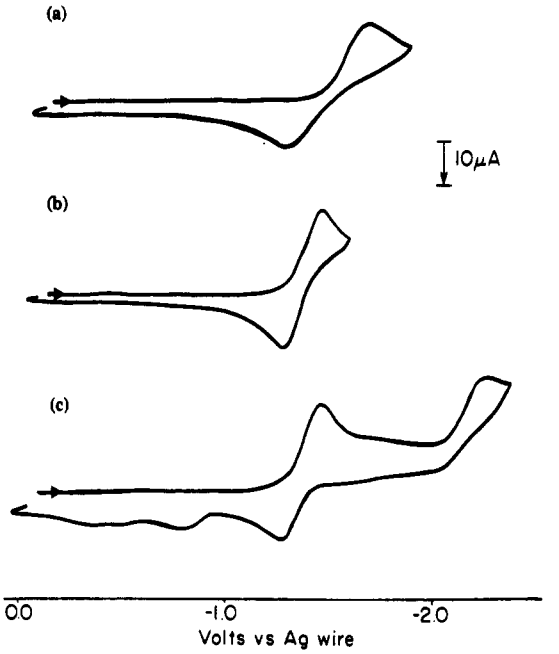

Figure 3. Ambient-temperature cyclic voltammograms (in THF, 0.10 N $[n\text{-Bu}_4N]PF_6$, Pt working electrode, scan rate 0.80 V s^{-1}): (a) **1** from 0.0 to −1.9 V; (b) **2** from 0.0 to −1.6 V; (c) **2** from 0.0 to −2.4 V.

occurs at $E^{\circ\prime}_1 = -1.38$ V; the linearity of the plot of $i_{p,c}$ vs $v^{1/2}$ establishes that this reduction is diffusion-controlled. Furthermore, comparison of the $i_{p,a}/i_{p,c}$ and ΔE values for this reduction with the internal Cp_2Fe/Cp_2Fe^+ reference indicates that it is reversible (Table VIII). The second reduction of complex **2** occurs at −2.18 V but is irreversible, thus implying that the compound is not retaining its structural integrity upon addition of the second electron.

Neither complex **1** nor **2** undergoes any oxidation processes up to the solvent limit of 0.80 V vs Ag wire. The small oxidation features evident in Figure 3c, but not in Figure 3b, may be attributed to reoxidation of the species formed by the irreversible reduction of **2** at −2.18 V (vide supra). With the information gleaned from this study, it seems that the preparation and isolation of $\mathbf{1}^{\bullet-}$ and $\mathbf{2}^{\bullet-}$ radical anions should be possible. It is equally clear that complex **1** does not undergo any bond-cleavage processes upon initial electron addition. Hence, it seems unlikely that its reactions with water involve any redox processes (vide infra).

Labeling Studies. A series of experiments were monitored by ^1H NMR spectroscopy in C_6D_6 in order to gain some mechanistic insights into the transformation of $Cp^*Mo(NO)(CH_2SiMe_3)_2$ (**1**) to $[Cp^*Mo(NO)(CH_2SiMe_3)]_2(\mu\text{-O})$ (**2**) by H_2O. The results of these experiments are summarized pictorially in Scheme I. Thus, treatment of **1** with excess water results in the clean conversion of **1** to **2** (~95% by ^1H NMR spectroscopy) with concomitant formation of 2 equiv of Me_4Si. The ^1H NMR spectrum also contains a small singlet at δ 1.78 ppm attributable to ~2% of $[Cp^*Mo(O)_2]_2(\mu\text{-O})$, which results from further hydrolysis of **2** (vide infra). Reaction of **1** with D_2O results in the synthesis of **2** but with DH_2CSiMe_3 being produced as the byproduct of the reaction. This byproduct is readily identified by the appearance of a singlet in the ^1H NMR spectrum at δ 0.00 ppm with a smaller 1:1:1 triplet (J_{HD} = 2.1 Hz), the latter signal being due to the monodeuterated methyl group of DH_2CSiMe_3. Taken together, these experiments clearly demonstrate that the water used to convert 2 mol of complex **1** to 1 mol of complex **2** ends up as 2 mol of Me_4Si (RH) and 1 mol

(30) Lincoln, S.; Koch, S. A. *Inorg. Chem.* **1986**, *25*, 1594.
(31) Carty, P.; Walker, A.; Matthew, M.; Palenik, G. J. *J. Chem. Soc. D* **1969**, 1374.
(32) Legzdins, P.; Rettig, S. J.; Sánchez, L.; Bursten, B. E.; Gatter, M. G. *J. Am. Chem. Soc.* **1985**, *107*, 1411.

Scheme I

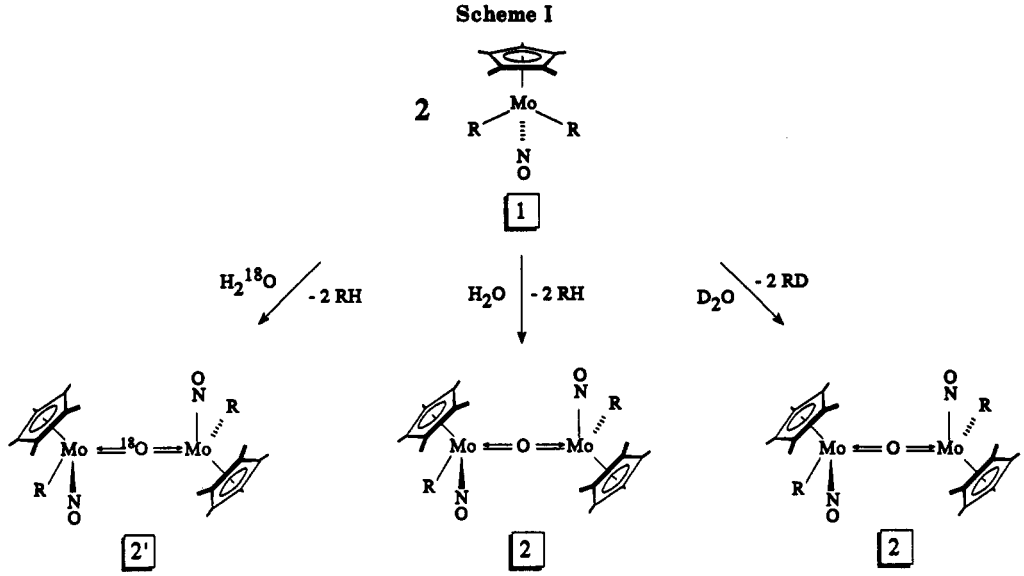

of complex 1. In other words, the balanced chemical equation for this transformation is as depicted in eq 8.

$$2Cp^*Mo(NO)R_2 + H_2O \rightarrow [Cp^*Mo(NO)R]_2(\mu\text{-}O) + 2RH \quad (8)$$

$$R = CH_2SiMe_3$$

Finally, treatment of 1 with $^{18}OH_2$ cleanly converts 1 to 2', the ^{18}O-labeled analogue of 2. This product may be conveniently characterized by mass spectrometry. The mass spectrum of 2' shows a parent ion peak at m/z 714 (as compared to 712 for unlabeled 2 recorded under identical experimental conditions).

The most plausible mechanistic pathways for reaction 8 to follow are presented in Scheme II. Water, a good Lewis base, could form an initial 1:1 adduct with the 16-electron dialkyl complex 1. Intramolecular expulsion of RH would afford the hydroxo alkyl intermediate A, which could function as a Lewis base toward a second molecule of 1 to form a bimetallic μ-OH complex. In the final step this latter compound could eliminate RH to form complex 2. Alternatively, the intermediate A could couple with another molecule of A to give the hydroxo dimer shown. Loss of H_2O from this dimer would then yield complex 2. In order to gain some further insight into the mechanism of this reaction, a kinetic analysis of reaction 8 was undertaken.

Kinetic Studies. A kinetic analysis of reaction 8 is hampered by several factors which merit explanation. The first is that the product of reaction 8, complex 2, undergoes further reaction with water and converts to [Cp*Mo-$(O)_2]_2(\mu$-O) (vide infra). The relative effect of this competitive and undesirable reaction is heightened at low concentrations of the organometallic starting material 1 and under pseudo-first-order conditions where water is in excess. The second factor is the difficulty of monitoring complex 1 as conversion 8 proceeds. For instance, our preliminary attempts to probe the kinetics of reaction 8 by ^1H NMR spectroscopy were unsuccessful. Since water is immiscible with benzene, it could not be used as a pseudo-first-order reagent in that solvent. In THF (a solvent with which water is miscible), the Cp* resonances for 1 (δ 1.84 ppm) and 2 (δ 1.86 ppm) are not sufficiently resolved to be integrated accurately. Furthermore, the signals in the spectral region around δ 0.00 ppm are not sufficiently resolved to permit monitoring of the Me_4Si byproduct. Consequently, we decided to effect a preliminary kinetic analysis of reaction 8 in THF using UV–vis spectroscopy, since complexes 1 and 2 exhibit different spectral properties (Table IX). The UV–vis spectra of 1 and 2 in THF are similar, except that 2 exhibits a strong band at λ_{max} = 404 nm, $\epsilon \approx 14000$ M^{-1} cm^{-1}. From a spectral overlay it is clear that monitoring of the disappearance of starting material would be very difficult, since no absorption band of 1 is sufficiently resolved from bands of the hydrolysis product 2. However, a Beer's law plot showed the absorptivity of 2 at 404 nm to be linear ($r^2 > 0.99$) up to A = 2.0, and so this spectral feature was monitored as the hydrolysis reactions progressed. Reactions were performed under pseudo-first-order conditions with an excess of water present. Because complex 2 does eventually react further with water to form [Cp*Mo-$(O)_2]_2(\mu$-O), the occurrence of this latter process was minimized by keeping the reactants as concentrated as possible within the linear absorption limits.

Table IX. UV–Visible Data for Complexes 1 and 2

complex (concn, M)	λ, nm	ε	A
1 (1.149×10^{-4})	223	14038	1.613
	300	7909	0.909
	526	752	0.086
2 (5.340×10^{-5})	236	60112	3.210
	276	58089	3.102
	404	13932	0.744

Under the experimental conditions employed, the progress of reaction 8 in THF is initially first-order in 1 since all plots of ln $(A_\infty - A_t)$ versus time are linear over an order of magnitude change in the concentration of 1, i.e. 2.56×10^{-4}–25.39×10^{-4} M. The concentration of water for the seven experiments defining the concentration range of 1 was held constantly in excess at 5.55×10^{-3} M. From plots of ln $(A_\infty - A_t)$ versus time, the average value of k_{obs} is 1.26×10^{-4} s^{-1} at 25 °C.[31] The calculated value of k from this dialkyl variation data gives $k = k_{obs}/[H_2O] = 1.26 \times 10^{-4}/5.55 \times 10^{-3} = 0.0227$ M^{-1} s^{-1} at 25 °C. At very low concentrations of 1 (i.e. $[1]_0 < 1.0 \times 10^{-4}$ M), plots of ln $(A_\infty - A_t)$ versus time are not linear, a feature which probably reflects that the conversion of 2 to [Cp*Mo-$(O)_2]_2(\mu$-O) by water becomes much more significant at very low concentrations of the organometallics.

The hydrolysis reaction (8) was also studied by varying the water concentration and keeping the initial concentration of 1 constant at 1.116×10^{-3} M. Thus, $[H_2O]$ was varied, but still kept in excess, in six experiments from 0.62 $\times 10^{-2}$ to 6.24×10^{-2} M. Under these conditions, the reaction appears to be first-order in water, since all plots

Scheme II

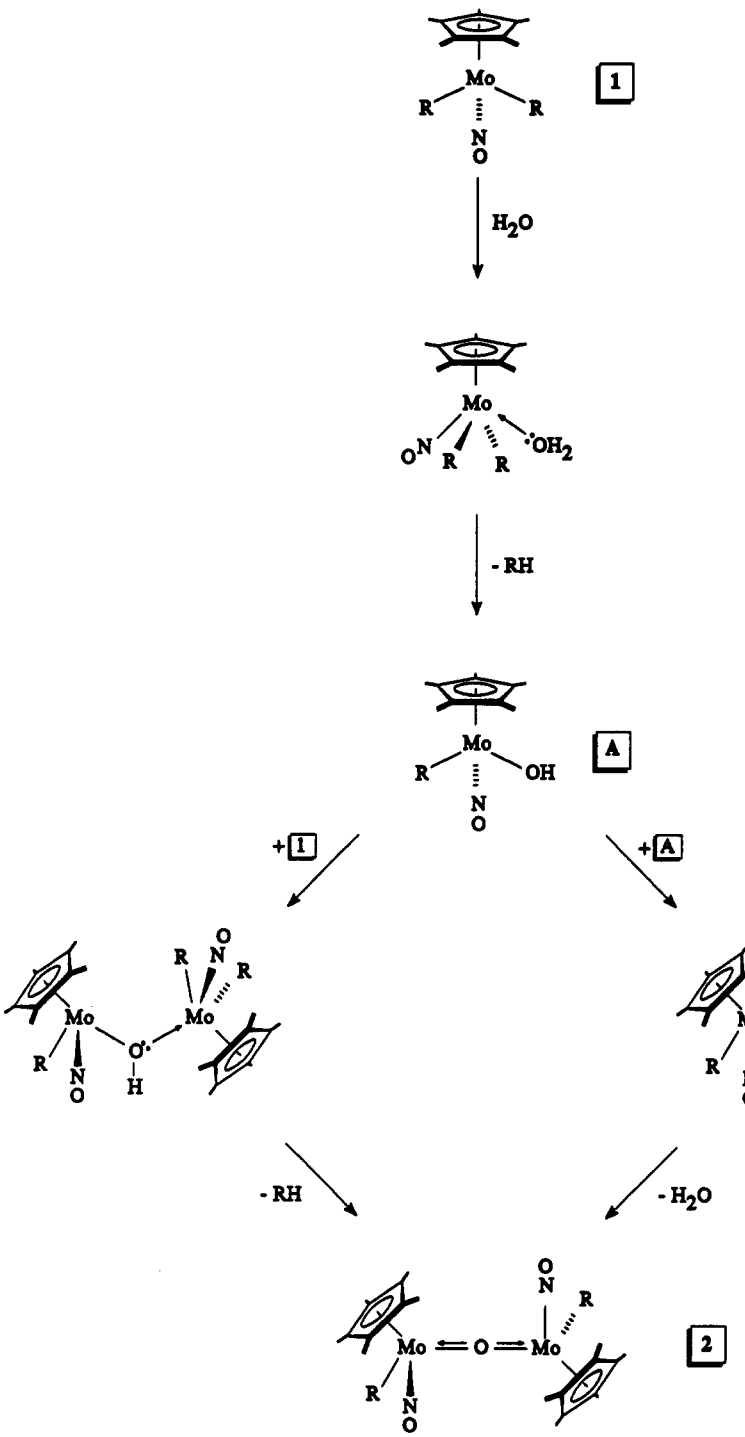

of ln $(A_\infty - A_t)$ versus time are initially linear. The kinetics of the reaction were also investigated at four temperatures between 15 and 30 °C. To check the validity of the variable-temperature data, a calculation of $k = k_{obs}/[H_2O]$ at 25 °C afforded a value of 0.0250 M^{-1} s^{-1}, in reasonable agreement with the value obtained from the dialkyl variation data (vide supra).

An Arrhenius plot of ln k_{obs} versus $1/T$ yields a straight line from which the activation energy, E_a, is calculated to be 49.0 kJ mol^{-1} and the preexponential factor A is 9.61×10^4. An Eyring plot of ln (k_{obs}/T) versus $1/T$ affords a straight line from which the following activation parameters may be calculated:[33] $\Delta H^\ddagger = 46$ kJ mol^{-1}, $\Delta S^\ddagger = -38$ eu, $\Delta G^\ddagger_{298} = 93$ kJ mol^{-1}. The sign and magnitude of $\Delta S^\ddagger$ clearly indicate that the rate-determining step of conversion 8 is highly associative in nature.

Finally, the hydrolysis reaction was also studied using D_2O instead of H_2O. Again, the reaction appears to be first-order with respect to D_2O, the average value of k_{obs} being 2.2×10^{-5} s^{-1}. The primary kinetic isotope effect (k_H/k_D) for the hydrolysis reaction is thus 0.0227/0.0040 = 5.7, suggesting the rate of the hydrolysis reaction being slowed substantially by using the heavier isotope. This observation is significant in that it suggests that there is a considerable degre of O–H bond breaking in the transition state.[34] This, in turn, is in accord with the reaction

(33) Moore, J. W.; Pearson, R. G. *Kinetics and Mechanism*, 3rd ed.; Wiley-Interscience: Toronto, 1981.

(34) For comparison, the maximum kinetic isotope effect, k_H/k_D, expected for breaking an O–H bond is 11.0 (see ref 33, p 369).

Scheme III

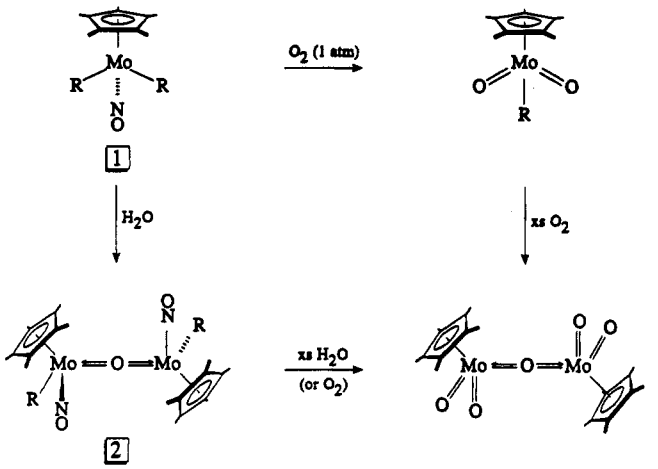

R = CH_2SiMe_3

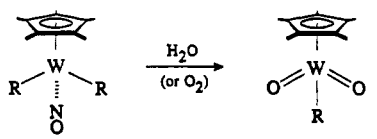

R = Ph (9), *p*-tolyl (10), *o*-tolyl (11)

proceeding via the intermediate alkyl hydroxo complex (A in Scheme II).[35] Regrettably, monitoring of the reaction in THF-d_8 by variable-temperature ^{1}H NMR spectroscopy (−80 to +20 °C) fails to detect any signals that could be attributable to anything other than 1, either isomer of 2, or Me_4Si. Therefore, although we cannot unambiguously determine the mechanism of the hydrolysis reaction, we can say that the rate-determining step is highly associative in nature ($\Delta S^{\ddagger}$ = −38 eu) and likely involves O–H bond breaking and Mo–O bond formation.

Comparisons of Reactivity. Scheme III summarizes the reactions of Cp*Mo(NO)$(CH_2SiMe_3)_2$ and its oxo derivatives with water and oxygen and illustrates the variety of products, both mono- and bimetallic, that may be obtained. To date we have isolated three compounds resulting from oxidation or hydrolysis of 1. As we have reported previously,[16] the dialkyl complex 1 reacts with dry O_2 to give Cp*Mo$(O)_2(CH_2SiMe_3)$ in moderate yield. In this paper we have described how 1 reacts with H_2O to provide high yields of 2. While Cp*Mo$(O)_2(CH_2SiMe_3)$ and 2 cannot be interconverted, both species do react with excess water or excess oxygen to form the known [Cp*Mo$(O)_2]_2(\mu$-O) complex as the only isolable organometallic product.[17] ^{1}H NMR monitoring of the reaction of 2 with a large excess of H_2O revealed the reaction to be nearly quantitative. Nevertheless, sagacious choices and careful execution of reaction conditions are necessary to obtain a particular oxo derivative of 1 experimentally. The reactions of 1 outlined in Scheme III appear to be quite general for the family of Cp'Mo(NO)R_2 (R = alkyl, aryl) complexes (vide supra).

In marked contrast, the reactions of Cp'W(NO)$(alkyl)_2$ with water and oxygen differ dramatically from those of their Cp'W(NO)$(aryl)_2$ analogues. The Cp'W(NO)$(alkyl)_2$ complexes resist reaction with water, persisting even in the presence of vast excesses of water for prolonged periods of time under ambient conditions. However, all Cp'W(NO)$(aryl)_2$ complexes that we have isolated to date[1] react instantaneously with water to form monometallic aryl dioxo complexes (Scheme III).[5] Finally, treatment of *both* Cp'W(NO)$(alkyl)_2$ and Cp*W(NO)$(aryl)_2$ species with O_2 affords *only* Cp'W$(O)_2$(alkyl) and Cp*W$(O)_2$(aryl) complexes via currently unknown mechanisms. The physical properties of the latter complexes (summarized in Tables I–III) are similar to those exhibited by their alkyl dioxo analogues.[16] Aryl dioxo complexes, however, tend to be less crystalline and less soluble in common organic solvents than their alkyl congeners, but they are equally air- and moisture-stable.

To the best of our knowledge, the fact that the molybdenum and tungsten dialkyl and diaryl species exhibit such different hydrolysis chemistry is unique. Typically, related compounds of the second- and third-row transition metals react in a similar manner, with the third-row compound being the slower to react.[37] Such is indeed the case for the hydrolyses of Cp_2MMe_2 (M = Zr, Hf). Thus, reaction of Cp_2MMe_2 with water in air leads to the formation of isoelectronic analogues of 2, namely $[Cp_2MMe]_2(\mu$-O).[38,39] Evidently, the differences created by changing the metal in related Cp'M(NO)R_2 (M = Mo, W) complexes have a much more pronounced effect on the characteristic chemical behavior of these species.[40]

The results summarized in Scheme III further confirm the generalization presented in the Introduction, namely that the characteristic chemical properties of Cp'M(NO)-containing complexes are very much dependent on the natures of the metal and the ancillary ligands. Further studies of these intriguing systems are in progress.

Acknowledgment. We are grateful to the Natural Sciences and Engineering Research Council of Canada for support of this work in the form of grants to P.L. We also thank Professor Brian James for helpful discussions.

Supplementary Material Available: Tables of calculated hydrogen coordinates, isotropic thermal parameters, final anisotropic thermal parameters, and torsion angles for [Cp*Mo(NO)$(CH_2SiMe_3)](\mu$-O) (17 pages). Ordering information is given on any current masthead page.

OM920266H

(35) It may be noted that Bercaw[36] has invoked an analogous hydroxo complex, namely $Cp^*_2Zr(H)(OH)$, as the intermediate species formed when $Cp^*_2Zr(H)_2$ and $Cp^*_2Zr(N_2)$ react with water. The ultimate product in these reactions is $[Cp^*_2Zr(H)]_2(\mu$-O), a valence-isoelectronic analogue of complex 2.

(36) Hillhouse, G. L.; Bercaw, J. E. *J. Am. Chem. Soc.* **1984**, *106*, 5472.

(37) "In general, the second and third transition series elements of a given group have similar chemical properties, but show pronounced differences from their light congeners.": Cotton, F. A.; Wilkinson, G. *Advanced Inorganic Chemistry*, 5th ed.; Wiley-Interscience: Toronto, 1988; p 776.

(38) Hunter, W. E.; Hrncir, D. C.; Bynum, R. V.; Penttila, R. A.; Atwood, J. L. *Organometallics* **1983**, *2*, 750.

(39) Fronczek, F. R.; Baker, E. C.; Sharp, P. R.; Raymond, K. N.; Alt, H. G.; Rausch, M. D. *Inorg. Chem.* **1976**, *15*, 2284.

(40) It has been noted that Zr and Hf complexes are more nearly identical than for any other two congeneric elements, mostly due to the lanthanide contraction (see ref 37, Chapter 19).